Rebuttal Expert Report
United States v. BP Exploration & Production, et al.
MDL 2179 (E.D. La.)

Analyses of MDT Pressure-Transient Data

Prepared by:

Leif Larsen
Myklabergstien 15
N4052 Royneberg
Norway

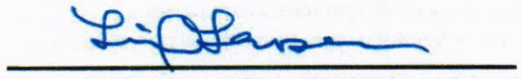

June 10, 2013

Table of Contents

1. PROFESSIONAL BACKGROUND

I am a Senior Reservoir Engineer with Kappa Engineering and an Adjunct Professor in Reservoir Engineering at the University in Stavanger, Norway. I have a PhD in mathematics from the University of California, Irvine. I joined the oil industry in 1980, and have since worked on development and implementation of mathematical solutions for use in well-test analyses and at the same time worked on analyses of field data. From 1980 to 1991 I worked at Rogaland Research Institute, from 1991 to 2007 I worked for Statoil, and since then as a consultant for Kappa Engineering, where I do analyses for clients and work on development and implementation of solutions in their software programs. In particular, I helped develop Kappa's module to analyze data from single and multi-probe tools. In 2007, while in Statoil, I was also part of a Statoil/Schlumberger team developing a new MDT tool with better gauge resolution and higher pump capacity, where my role involved criteria for obtaining acceptable data from high-mobility formations.

I have analyzed data from a large number of wire-line runs, especially from the Norwegian Continental Shelf, with tools from different vendors. I have also worked on MDT data from the Gulf of Mexico based on the same type of tool run in the MC252 well, but with better test data from formations with poorer properties.

I have served on several SPE committees, was an SPE distinguished lecturer 1998-99, and the 2012 recipient of the SPE Formation Evaluation Award. A true and correct copy of my current curriculum vitae is attached as Appendix A to this report.

2. MY OPINION

I have carried out new analyses of the MDT test data from the wire-line run April 12, 2010 in the MC252 well with the objective of determining whether Dr. Gringarten's analysis of the same data is credible. In doing so, I attempt to estimate the formation permeability of the M56D, Upper M56E and Lower M56E sands. My estimates differ clearly from those presented by Dr. Gringarten[1] for the two best sands, but is in general agreement for the sand with the lowest flow capacity – the Upper M56E sand. Our agreement on the permeability of the lowest flow capacity sand is consistent with my experience and the literature indicating that estimating permeability with MDT data is more reliable for lower

[1] Expert report of A. Gringarten.

permeability sands. The differences for the best sands are caused by different methodologies used to analyze the data, with Gringarten relying on data smoothing, semi-log derivatives and de-convolution in his analyses,[2] while I have based my analyses directly on recorded data and comparisons with data computed from a proper single-probe model.[3]

2.1. Uncertainties in the Data

Before turning to my analysis of the MDT data, it is important to note several limitations of the data. The data under consideration are very noisy and limited. This noise is particularly significant with respect to the M56 Reservoir because this reservoir is one with high mobility – that is the reservoir has a high ratio of permeability to fluid viscosity. As noted above, I have worked with MDT data from the Gulf of Mexico based on the same type of tool run in the MC252 well, but in those cases I had better test data from formations with lower mobility.[4]

In the tests under consideration, the MDT data exhibit rapid pressure recoveries after shut-ins. Rapid pressure recoveries imply rapid pressure stabilization. This adds uncertainty to analyses when the pressure changes approach or fall below the resolution of the gauge, with signal noise and operational disturbances then limiting the reliability and usefulness of the data.

Another limitation on the MDT data in question is that the test was designed for fluid sampling and to take pressure points, not to generate data for formation testing.[5] This is the normal use of the MDT tool, to collect down-hole fluid samples and to take pressure points. This is clearly reflected in in the Macondo data, with pump schedules optimized for sampling – and not for formation testing. The changing pump schedules and dual-pump operations used for the Macondo MDT sampling added effects in the data that make use of these data in well-test analyses challenging.

2.2. My Results

Given the data constraints, I have made a best effort to estimate the likely range of permeability of the sands in question. By this approach I need to determine a robust mean value for each sand, referred to as my best "single-value estimate," along with a realistic

---

[2] Expert report of A. Gringarten, pages 27 and 28.
[3] Larsen, L.: "Modeling and Analyzing Source and Interference Data From Packer-Probe and Multiprobe Tests," paper SPE 102698 presented at the SPE Annual Technical Conference and Exhibition, San Antonio, Texas, 24–27 September 2006.
[4] See Larsen, L.: "Modeling and Analyzing Source and Interference Data From Packer-Probe and Multiprobe Tests," paper SPE 102698 presented at the SPE Annual Technical Conference and Exhibition, San Antonio, Texas, 24–27 September 2006, page 6.
[5] Emanuel Dep. at 27-29.

range based on possible upper and lower limits. In my analyses I took the basic parameters of net thickness, porosity, viscosity and total compressibility from Dr. Gringarten's report. These have negligible impact on my analyses of MDT data in the sense that realistic changes will not have a significant impact on my results, if any.

Using these parameters, I get the results listed in Table 1, with my best single-value permeability estimate 500 md for the M56D sand, 150 md for the Upper M56E sand and 500 md for the Lower M56E sand. These results are consistent with core and log-based data described in a BP Technical Memorandum dated July 26, 2010.[6] The same estimates (P50) presented by Gringarten[7] are 116 md (M56D), 117 md (Upper M56E) and 285 md (Lower M56E). See Table 2. Although our estimates for the Upper M56E are in general agreement, I believe that Gringarten substantially underestimates the permeability of the M56D and Lower M56E sands.

Table 1 – Input and derived parameters from the MDT data.

Sand unit	M56D	Upper M56E	Lower M56E
Data file	F144	F143	F147
Net thickness, ft	22	15.4	49.1
Porosity	0.207	0.221	0.221
Viscosity, cp	0.243	0.243	0.243
Total compressibility, 1/psi	17.8E-6	18.6E-6	18.6E-6
Horizontal permeability, md [1]	500	150	500
Vertical permeability, md [2]	50	15	50
Total cumulative flow, bbls	1.07	0.92	1.23
Radius of investigation, ft [3]	137	68	120
Formation pressure, psia	11841.09	11850.58	11855.77
Probe depth, ft MD	18085.97	18123.93	18142.00

1) The values listed are my best single-value permeability estimates
2) The results do not depend strongly on the vertical permeability, but low horizontal permeability tend to require a higher k_V/k_H ratio, which can be unrealistic
3) Horizontal distance listed from the longest buildups

The thickness-based average permeability of the three sands will be 438 md. In my view this is a conservative (low) estimate. The value reported by Gringarten is 238 md.[8] That number substantially underestimates the effective permeability of the reservoir.

[6] BP-HZN-BLY00082874.
[7] Expert report of A. Gringarten, pages 30 and 31.
[8] Expert report of A. Gringarten, page 25.

Table 2 – Comparison of My Estimates to Dr. Gringarten's		
Sand Unit	My Estimate	Dr. Gringarten's Estimate
M56D	500 md	116 md
Upper M56E	150 md	117 md
Lower M56E	500 md	285 md
Thickness Based Average	438 md	238 md

2.3. Additional Critique of Dr. Gringarten's Methodology

I have at least two additional significant critiques of Dr. Gringarten's approach in his report.

First, Dr. Gringarten used a standard well model with a short open interval in his analyses.[9] This approach should be combined with a small effective wellbore radius to be realistic in comparison with flow to the tool through a small hole in the mud-cake on one side of the wellbore. Since the effective wellbore radius is modified from the actual radius by the factor exp(-skin) in the model, the skin value has to at least exceed 1, corresponding to a reduction by a factor of exp(-1) = 0.37, for the model to be realistic. In the case shown in his Fig. 12,[10] Dr. Gringarten matches the data from M56D with a permeability of 110 md and skin values near 0. This shows this low permeability to be unrealistic. In Fig. 12[11] the same data are matched with a permeability of 292 md and skin values around 0.5. These low skin values imply that this permeability has to be considered as a low estimate. The same comments apply to Dr. Gringarten's analyses of the Lower M56E data, with Fig. 34[12] showing that even negative skin values have been used, implying a tool diameter larger than the wellbore, for his low case at 101 md, and that skin values around 0.5 have been used for his high case at 240 md. These skin values show that 240 md can only be treated as a low estimate for the Lower M56E sand, with 101 md not being meaningful.

Second, Dr. Gringarten used data smoothing and deconvolution to analyze the data, thereby basing his analyses on modified data. With high mobility and low rates, gauge resolution, signal noise and operational disturbances reducing the quality of MDT data, data smoothing is inappropriate because there are too few points for such algorithms to work properly. The problem is that smoothing will by design reduce noise in the data and allow semi-log derivatives (trends) to be computed directly from the modified data with the true information of the data easily lost in the process. Since log-log plots can only display positive derivatives, the results will be biased towards high values for poor resolution and noisy data,

[9] Expert report of A. Gringarten, Appendix E, page 29.
[10] Expert report of A. Gringarten, Appendix E, Fig. 12, pages 9 and 10.
[11] Expert report of A. Gringarten, Appendix E, Fig. 13, page 11.
[12] Expert report of A. Gringarten, Appendix E, Fig. 34, page 27.

even after smoothing, with an upward swing in derivatives at "late" times often seen in such data sets. Derivatives with this behavior, which is an artifact of semi-log derivatives computed from sparse data sets with poor resolution, should therefore not be used in analyses, but Dr. Gringarten honored such data in some analyses,[13] thereby underestimating permeability, and even interpreted such behavior as representative of nearby flow barriers (wedge model).[14]

Dr. Gringarten's use of deconvolution is similarly inappropriate. Deconvolution is a method to determine a pressure-response as a function of time with certain constraints. The goal of this analysis is to reproduce an ideal test response for flow at constant rate throughout the entire test sequence. In essence, this means a pressure response established from a short buildup is extended to the entire test sequence by honoring an assumed or observed pressure drop through the data set, e.g., from the first to the last buildup. For the Macondo data with very small pressure changes, the key pressure drop needed in the analysis cannot be determined with sufficient certainty. In fact, for the data sets at hand, the observed trend in the deconvolved data beyond the length of key buildups will actually be controlled by the assumed pressure drop.

3. THE MDT TOOL

A dual-pump, single-probe module was used in the sampling run when the three data sets used in well-test analyses were collected from the MC252 well.[15] The dual pump was used with a focused probe as shown at the right in Figure 1, with two concentric probes (tubes) used to withdraw fluid from the formation. The sampling took place in the open-hole section at the bottom of the well with wellbore radius 0.354 ft. Communication with formation fluid in such operations is established by pushing a packer-and probe assembly against the mud-cake on one side of the borehole with a single or double probe (tube) penetrating the mud-cake and reaching the formation. A full view of the tool without the opposite side hydraulic pistons used to establish force against the mud-cake and the formation is shown in Figure 2 along with a schematic of fluid flow.

[13] Expert report of A. Gringarten, Fig. 14, page 12.
[14] Expert report of A. Gringarten, Fig. 34, page 27.
[15] See the Schlumberger MDT Report, May-09-2010, pages 29, 31-33 and 34

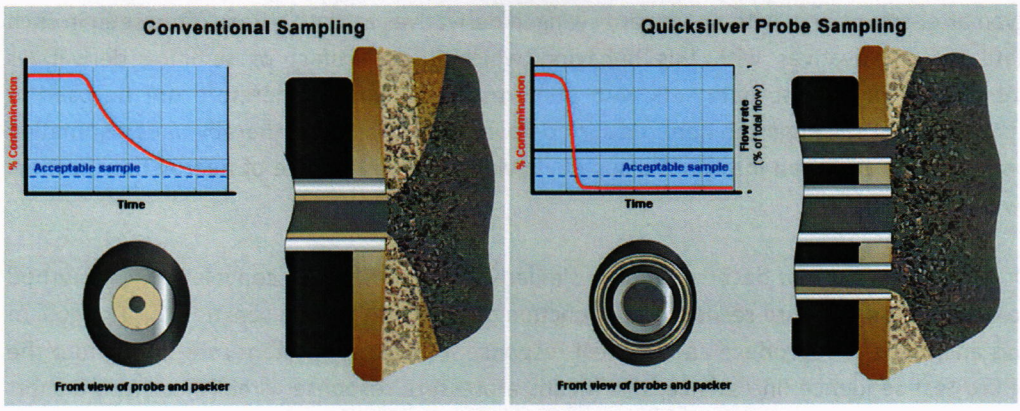

Figure 1 – Conventional and dual-pump probes with typical contamination-time plots. In the right schematic, filtrate-contaminated fluid is contained by the annular perimeter probe (guard pump) while the center probe (sample pump) extract near contamination-free reservoir fluid (copied from Schlumberger brochure).

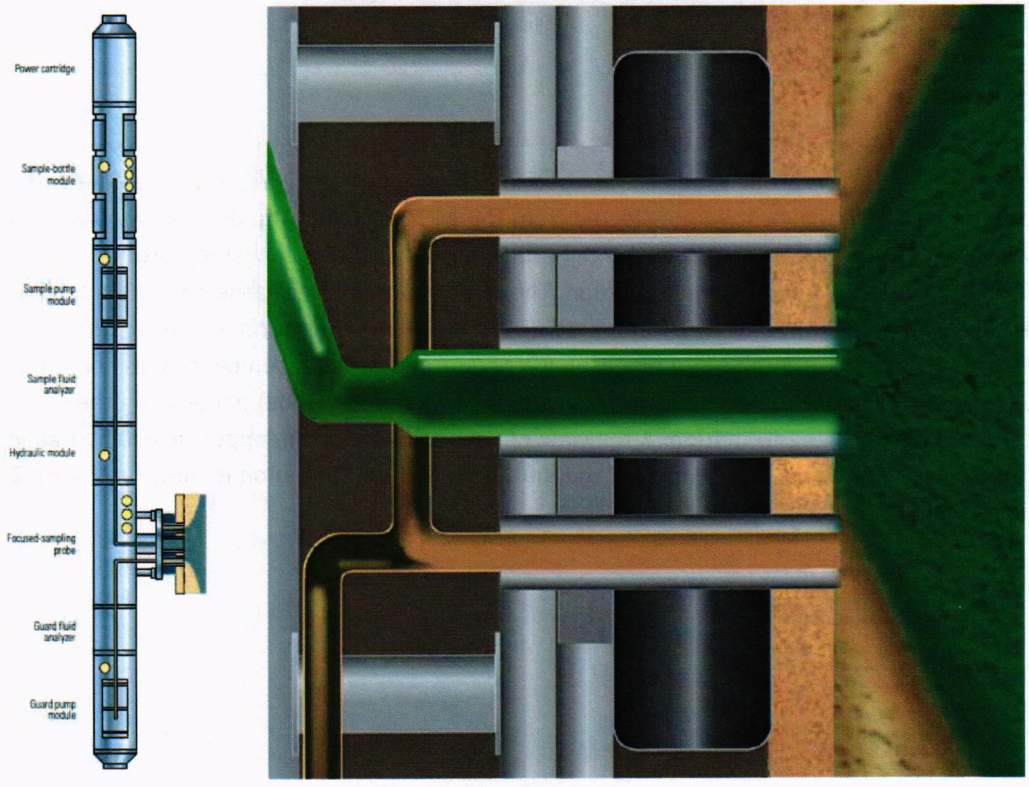

Figure 2 – Overview of the dual-pump module without the opposite side pistons used to establish hydraulic force against the formation, together with a schematic of the fluid flow with both pumps operating (copied from Schlumberger brochure).

The tool set-up is important because the flow pattern into the probe changes depending on whether both pumps are operating, just the sample pump (inner) or just the guard pump (outer perimeter). With a smaller probe diameter a larger pressure drawdown is created at a given rate. If both pumps are operating there is also more area and less flow-convergence effects than if just the outer (perimeter) probe is open to flow. Differences are therefore observed depending on how the pumps are operated.

The MDT tool is mainly used to collect down-hole fluid samples and to take pressure points. The pressure points are obtained with limited fluid withdrawal (around 20 cm^3) over periods of around 10-20 sec. Fluid sampling with the pump-out module, as was used in the Macondo well, is different, with fluid pumped over longer time periods through the tool and into the wellbore (mud column) with continuous recording of fluid properties. When acceptable cleanup is indicated from tool instruments, a sample bottle can be filled and sealed in the tool. This procedure can be repeated. The dual-pump module with focused sampling from the center of the fluid stream will normally greatly reduce time and improve the quality of samples. For the pressure data recorded during pumping and shut-in periods, the dual-pump operations can easily add effects in the data that make use of these data in well-test analyses challenging. The problem is that the pressure response is affect by the changing split in total flow rate between the inner and outer probe openings. The changing pump schedules are dictated by the sampling operations, and therefore planned.

4. PROBE MODEL USED IN ANALYSES

Since flow enters the tool from the formation through a single hole or a concentric double-hole in a no-flow cylindrical wellbore wall (the mud-cake), the model set-up sketched in Figure 3 is needed to analyze the test data, at least if both the overall drawdown and trends observed in the data are going to be used.

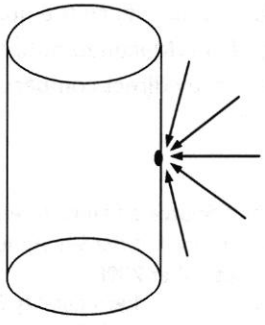

Figure 3 – Flow to a probe opening on a cylindrical no-flow wellbore wall (mud-cake).

The asymmetric model with flow pattern indicated in Figure 3 has been used in all analyses presented in this report. This model, which is described in detail in the paper SPE 102698,[16] (Larsen, 2006) is based on a solution presented by Goode and Thambynayagam[17] in 1992. 297.

As was discussed above, Dr. Gringarten used a standard well model with a short open interval in his analyses.[18] This is acceptable if a small wellbore radius is used or a positive skin value is obtained from the analysis, in essence implying a small effective wellbore radius. With a small wellbore radius and short interval open to flow a reasonable approximation of the actual flow behavior near the probe can be obtained, but not with near zero or negative skin values. This is important because the model used in an analysis with chosen permeability must match both the trend during shut-ins and the drawdown during flow periods. Again, as was pointed above, for some of his cases with low permeability Dr. Gringarten needed to use an unrealistic well model to match flow data,[19] and therefore should have eliminated those cases.

5. SHORT SUMMARY OF ANALYSES

Since the Macondo data come from a high-mobility formation, the use of an asymmetric single-probe model is not critical for analyses of pressure trends, but it does allow us to consider if the observed drawdown is consistent with the tool configuration. I have used this repeatedly in the detailed analyses in the following chapters, but the summary here is concentrated on direct matching of observed pressure trends during shut-ins.

From operational constraints, time on station is limited, and lengthy test sequences therefore not an option. The periods with shut-in data typically used in analyses are therefore short, and even with 1 recording per second, as in the Macondo data sets, periods of interest have few data points. With high mobility and low rates, gauge resolution, signal noise and operational disturbances tend to reduce the quality of MDT data. This fact cannot be amended with data smoothing of the Macondo data since there are too few points for algorithms to work properly. However, by direct comparison of actual data and model data

---

[16] See Larsen, L.: "Modeling and Analyzing Source and Interference Data From Packer-Probe and Multiprobe Tests," paper SPE 102698 presented at the SPE Annual Technical Conference and Exhibition, San Antonio, Texas, 24–27 September 2006.
[17] See Goode, P.A. and Thambynayagam, R.K.M.: "Permeability Determination With a Multiprobe Formation Tester," SPEFE (December 1992) 7, No. 4, 297.
[18] Expert report of A. Gringarten, Appendix E, page 29.
[19] Expert report of A. Gringarten, Appendix E, Fig. 34, page 27.

in different plots one can determine if these are close, i.e., if the model response matches the recorded data.

The point made above about smoothing only refers to shut-in periods. For periods with flow one can use various algorithms to smooth the data, but one can also manually remove outliers to obtain a cleaner data set. The latter is the approach I have used to avoid false trends, although these periods are not used directly in analyses and hence do not have any impact on results. The outliers being removed are mostly caused by pump strokes (reversals) and carry no information to analyses. These points have only been removed to avoid a wide pressure-signal band in data displays. Details about this approach are shown for the M56D data in the detailed analyses below.

The first of my analyses of M56D data is shown in Figure 4. This analysis is based directly on a semi-log plot of observed data from Buildup 4 (BU 4) and data generated by the probe model with horizontal permeability 500 md and vertical permeability 50 md. The initial pressure from this early buildup is 11841.07 psia and the skin value -0.12. With a reference probe diameter of 2 inches used throughout all analyses in this report, this implies an effective probe diameter of 2*exp(0.12) = 2.25 inches. This is the meaning of "skin value" S in this model in the sense that it is only used to modify the reference probe diameter by the factor exp(-S). Although the actual probe opening can be smaller, communication with the formation can be better than predicted by the model if for instance the permeability at the probe location happens to be higher than the average value over the formation. This can be seen as in improvement (negative skin).

By basing analyses directly on recorded data as shown in Figure 4, I can conclude that the permeability cannot be much lower than 500 md, since a permeability of 250 md would generate a steeper trend in the model, with a doubling towards the end. Higher permeability will do the opposite, and generate a shallower trend in the model data.

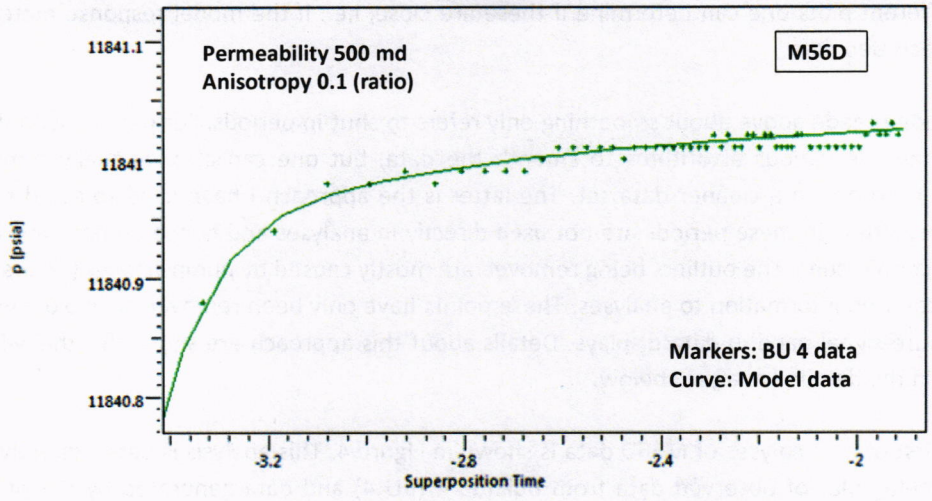

Figure 4 – Semi-log match of M56D data from BU 4 based on a single-probe model with horizontal permeability 500 md and vertical permeability 50 md.

An alternative to the approach above is to use a log-log plot of pressure changes after shut-in and slopes computed from the observed data in the semi-log plot, as shown in Figure 5. However, with the scatter seen in the data the slopes (semi-log derivatives) cannot be computed in a point-by-point procedure, and must be based on some smoothing of the data. However, with few data points and significant noise in the data, any form of smoothing will tend to be unreliable. Working directly with the data in semi-log plots is more robust.

Note that the high values of semi-log derivatives shown in Figure 5 is an artifact of gauge resolution and the fact that recorded values have been used directly. The point is that the horizontal axis in the semi-log plot compresses the time steps with increasing elapsed time (points closer together) while the minimal possible change in the pressure data remains fixed. Small derivatives consistent with the model data are therefore at best obtained by chance. If an algorithm had been used upfront to smooth the data, then the resolution would be reduced and this effect reduced. However, unless the modified data after smoothing come close to a smooth model response, the derivatives will still tend to included too high values at the end as an artifact of the use of few points and a non-negligible resolution (real or modified). Gringarten used log-log plots with derivatives in his analyses after an upfront smoothing of the data.[20] Even with reduced resolution in his data after smoothing, increasing derivatives towards the end of shut-ins are still observed, and has to be artifact of differentiation with improper data.

[20] Expert report of A. Gringarten, pages 27 and 28.

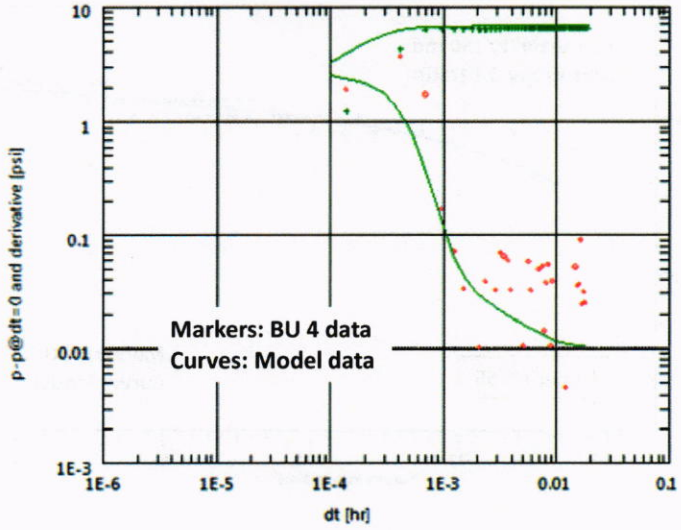

Figure 5 – Log-log match of the BU 4 data from the previous figure.

As for de-convolution, this is a method where a pressure-response function of time with certain constraints is determined with the objective to represent an ideal test response at constant rate throughout the entire test sequence. In essence, this means a pressure response established from a short buildup is extended to the entire test sequence by honoring an assumed or observed pressure drop through the data set, e.g., from the first to the last buildup. For the Macondo data with very small pressure changes, the key pressure drop needed in the analysis cannot be determined with sufficient certainty. In fact, for the data sets at hand, the observed trend in de-convolved data beyond the length of key buildups will actually be controlled by the assumed pressure drop.

The next of my key analyses is shown in Figure 6 as a semi-log match of data from BU 12 from the Upper M56E sand based on a single-probe model with horizontal permeability 150 md, vertical permeability 15 md, and a reference probe diameter of 2 inches. In this analysis, which is based directly on recorded data without smoothing or use of modified data, I have used a skin value of -0.25, which corresponds to an effective probe diameter of 2.6 inches. Additional analyses and plots can be found in the chapter covering detailed analyses of data from the Upper M56E sand.

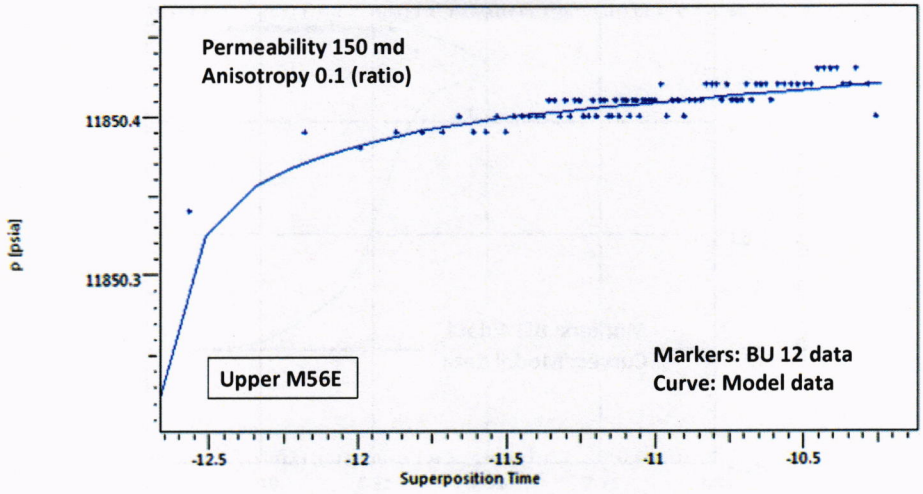

Figure 6 – Semi-log match of Upper M56E data from BU 12 based on a single-probe model with horizontal permeability 150 md and vertical permeability 15 md.

The analysis above is based on the data from the pre-test, with rate 0.91 B/D, which is less than half the value assumed to yield acceptable data. Still, the match, in Figure 6 is quite robust, with significant changes not realistic. Actually, due to a limited drawdown observed in the data, reducing the permeability is difficult without an unrealistic skin value. The analysis above is therefore my best estimate for the Upper M56E sand. My permeability of 150 md is also close to the P50 value 117 md listed by Gringarten.[21]

The last of my key analyses is shown in Figure 7 as a semi-log match of data from BU 3 data from the Lower M56E sand based on a single-probe model with horizontal permeability 500 md, vertical permeability 50 md. In this match I have used a skin value 0.55, which corresponds to an effective probe diameter of 1.2 inches. I have also based this analysis directly on recorded data without smoothing and use of modified data. Additional analyses and plots of data from the Lower M56E sand can be found in the chapter covering detailed analyses of Lower M56E data below.

For this data set the criteria for quality data are clearly violated, but the match is still fairly robust in the sense that significant changes would reduce the visual quality of the match. For instance, with permeability approaching 250 md an inconsistency with the data can be observed. There is also another limitation on low estimates, with permeability 250 md the vertical permeability must be high match a rapid pressure recovery in the data, but a high k_V/k_H ratio is not realistic for these formations.

[21] Expert report of A. Gringarten, page 31.

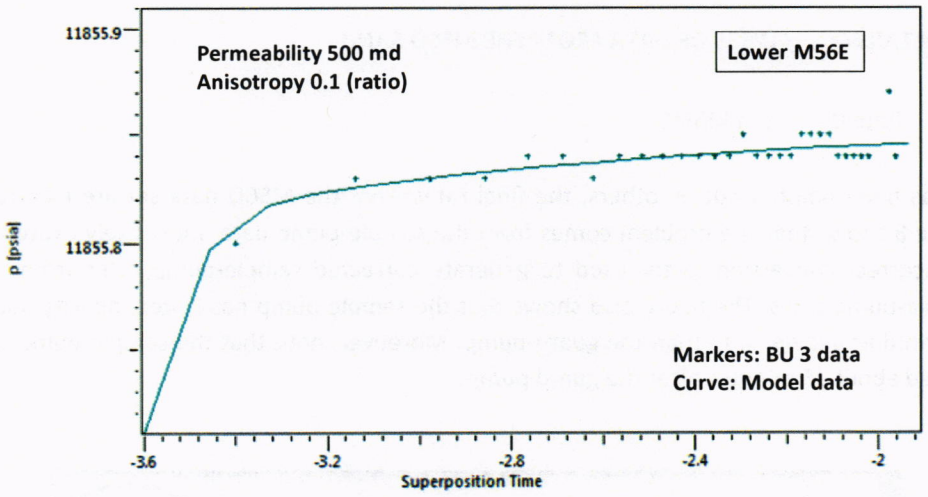

Figure 7 – Semi-log match of Lower M56E data from BU 3 based on a single-probe model with horizontal permeability 500 md and vertical permeability 50 md.

6. DETAILED ANALYSES OF DATA FROM THE M56D SAND

6.1. Rate Data from M56D

As has been pointed out by others, the final rates from the M56D data set are incorrect. Figure 8 shows that the problem comes from the sample-pump data, most likely caused by an incorrect conversion factor used to generate corrected sample-pump rates from raw sample-pump rates. The figure also shows that the sample pump has lower capacity and is operated at a lower rate than the guard pump. Moreover, note that the sample pump was started about 15 minutes after the guard pump.

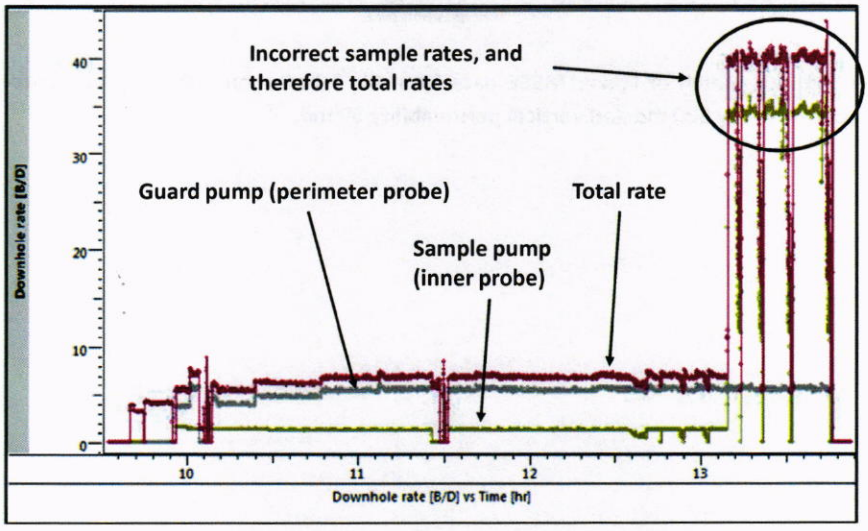

Figure 8 – Overview of the rate data from M56D, with obvious erroneous sample rates at the end of the data set.

Figure 9 highlights the observation above asserting that the incorrect rates come from an error when corrected sample-pump rates are generated from raw sample-pump rates. From the figure it also follows that the corrected rates are lower than the raw data since pump efficiency is lower than 100%. The same is true for the guard pump (not shown).

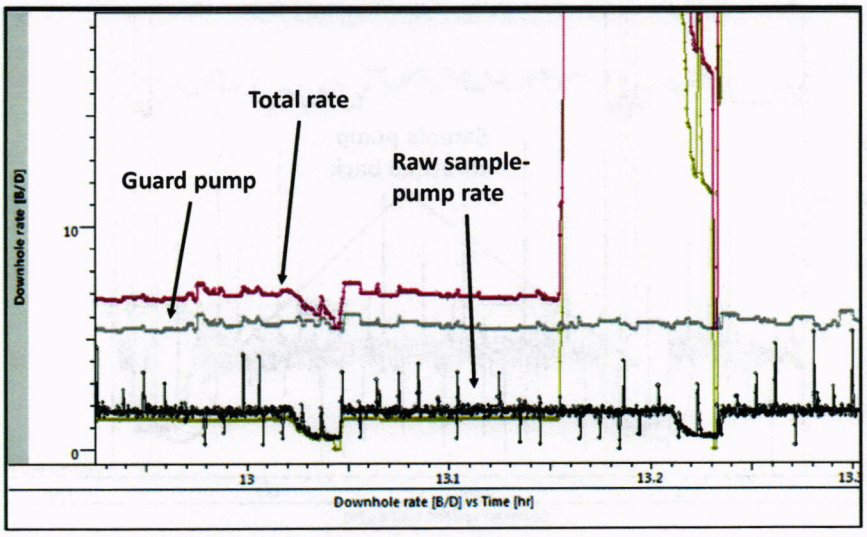

Figure 9 – Detail of M56D rate data showing the start of incorrect sample-pump rate registrations.

Of direct relevance for analysis of the final production test buildup in the M56D data, prior to the pre-test at the end of the data set, are the rates shown in Figure 10. This plot covers a period with incorrect total rates listed in the M56D data set. By comparing with earlier sample-pump data I have concluded that the sample pump was throttled back from 1.35 B/D (barrels per day) to zero for a period and then brought back up to 1.35 B/D. Added to the guard-pump rate of 5.8 B/D I therefore get a total rate of 7.15 B/D prior to shut-in.

The gradual reduction of sample-pump rate is also seen at other times. This procedure is related to fluid-sampling operations.

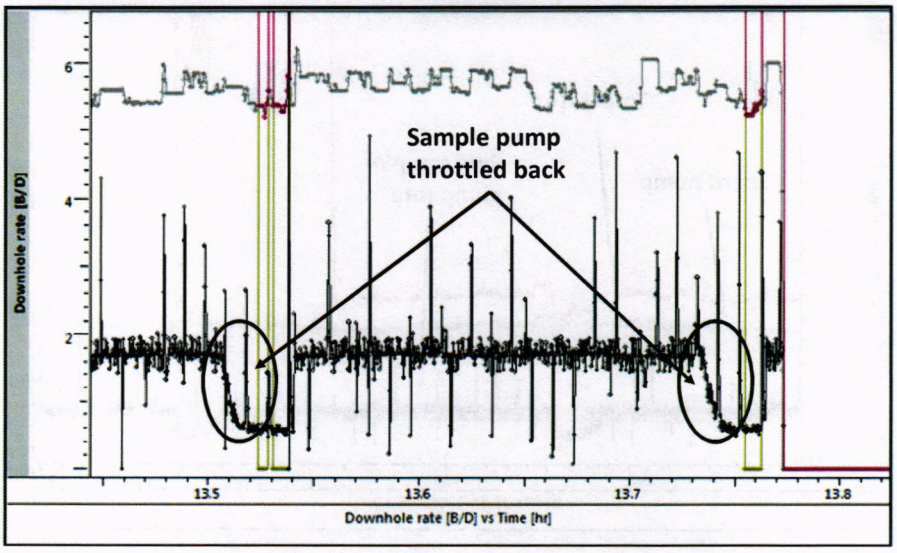

Figure 10 – Detail of the last part of the M56D rate data showing the sample pump to be stopped briefly before the last flow sequence prior to the final "production test" shut-in.

6.2. Pressure Data from M56D

Since the MDT data being analyzed come from high-mobility formations, and the test rates of the tool are relatively small, it is not appropriate to use standard well-test methods based on data smoothing, log-log diagnostic plots, or newer techniques such as de-convolution. Such methods should at least be used with great care. Instead, I have used more traditional treatment of the data along with the single-probe model described above to model and analyze the pressure response of the MDT tool.

From operational constraints, time on station is limited, and lengthy test sequences therefore not an option. The periods with shut-in data typically used in analyses are therefore short, and even with 1 recording per second, as in the Macondo data sets, periods of interest have few data points. When data are extracted from the log file (DLIS format) for use in analyses, e.g. as LAS files, one can over-sample the data by interpolation, but this will introduce false information and hence should be avoided.

With high mobility and low rates, gauge resolution, signal noise and operational disturbances tend to reduce the quality of MDT data. This fact cannot be amended with data smoothing of the Macondo data since there are too few points for algorithms to work properly. However, by direct comparison of actual data and model data in different plots one can determine if these are close, i.e., if the model response matches the recorded data.

The point made above about smoothing only refers to shut-in periods. For periods with flow one can use various algorithms to smooth the data, but one can also manually remove outliers to obtain a cleaner data set. The latter is the approach I have used to avoid false trends, although these periods are not used directly in analyses and hence do not have any impact on results. The outliers being removed are mostly caused by pump strokes (reversals) and carry no information to analyses. These points have only been removed to avoid a wide pressure-signal band in data displays.

Figure 11 illustrates the point above about data quality during shut-in periods. The data set is complete during the pre-test buildup at the end of the M56D data set in the sense that no pressure points have been excluded between the first and last within the ringed-in data, but some pressures have been excluded during the preceding period to focus on the resolution of the recorded pressure data. Part of the disturbances prior to the pre-test buildup, which are more severe than those shown, are most likely caused by preparations to run the pre-test.

Although it is easy to see that the pressures are indeed building up during the pre-test buildup, the trend is not obvious. If the data had been displayed with one more digit (one more decimal place), then it would have been easier to identify the trend even though the signal noise is greater than the resolution 0.01 psi of the recorded data. However, the situation about gauge, or data, resolution is better for the other buildups in the M56D data set since the rate is higher prior to these. The reason is that the pre-test is based on withdrawing roughly 20 cm^3 of fluid at a rate of about 1 cm^3/s, which corresponds to a rate of a little over 0.5 B/D. The rates prior to the other buildups are at least 10 times higher. This is important since the pressure response is directly proportional with the rate.

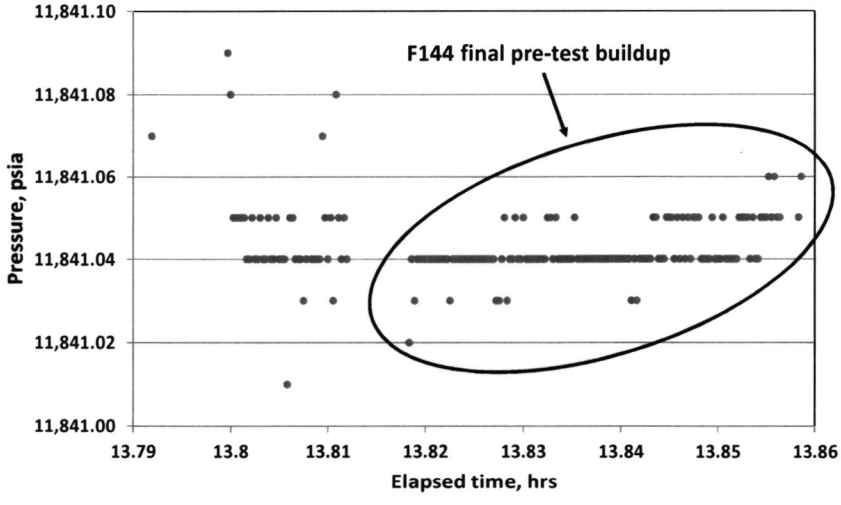

Figure 11 – Illustration of gauge resolution limitation, signal noise and operational disturbances at the end of the M56D data set.

Although not critical for analyses, pressure outliers caused by disturbances from the pumps have been removed to get a cleaner data set for use in data displays. This point is illustrated in Figure 12 with kept data shown in red and discarded data shown in turquoise. The excerpt of the data included in Figure 13 shows that the discarded data are indeed caused by pump strokes. These play no role in analyses, and hence can be removed without any loss of information or impact on results.

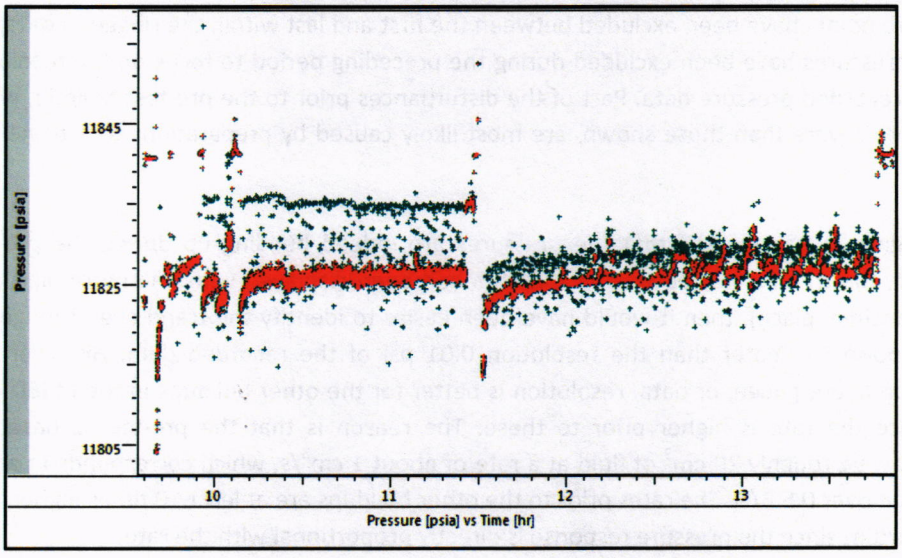

Figure 12 – The M56D pressure data showing kept data (red) and discarded data (turquoise).

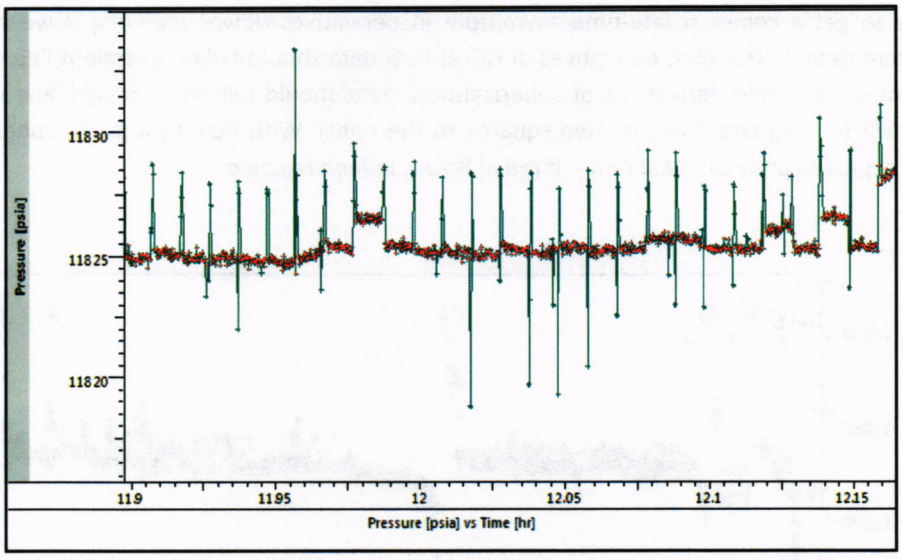

Figure 13 – Detail of the M56D pressure data showing the discarded data to represent pump-stroke effects.

The other issues I have brought up above, about pressure derivatives and de-convolution, will be discussed during relevant analyses. Note that pressure derivatives, or slopes in a plot of pressure or pressure changes versus a special semi-logarithmic super-position time scale, is the main source of identifying periods with radial flow. Periods with radial flow are critical, because such periods are the key sources of data to determine formation permeability. However, for data sets of the type ringed-in in Figure 11, software-based determination of point-by-point trends cannot be trusted off hand. Results must be verified by considering the data directly.

As for de-convolution, this is a method were a pressure-response function of time with certain constraints is determined with the objective to represent an ideal test response at constant rate throughout the entire test sequence. In essence, this means a pressure response established from a short buildup is extended to the entire test sequence by honoring an assumed or observed pressure drop through the data set, e.g., from the first to the last buildup. Due to cleanup effects and changing pump configuration, drawdown data from M56D cannot be used in this process. Moreover, due to changes from cleanup effects, the key pressure drop needed in the analysis cannot be determined with sufficient certainty. In fact, for the data sets at hand, the observed trend in de-convolved data beyond the length of key buildups will actually be controlled by the assumed pressure drop.

Figure 14 shows an overview of the complete M56D data set with 6 buildups identified. The standard approach used in well-test analyses is to plot pressure changes and semi-log derivatives from buildups in a log-log diagnostic plot, and to use this plot to identify flow regimes in the data. Figure 15 shows such data from all 6 buildups normalized with respect

to rate to get a common late-time asymptote in derivatives (lower markers) if we have consistent data. In this plot, derivatives of radial-flow data should fall on a straight line with constant value, while derivatives of spherical-flow data should fall on a straight line with slope -1/2 (one square down by two squares to the right). With flow to a point, spherical flow is expected prior to radial flow – if radial flow is indeed reached.

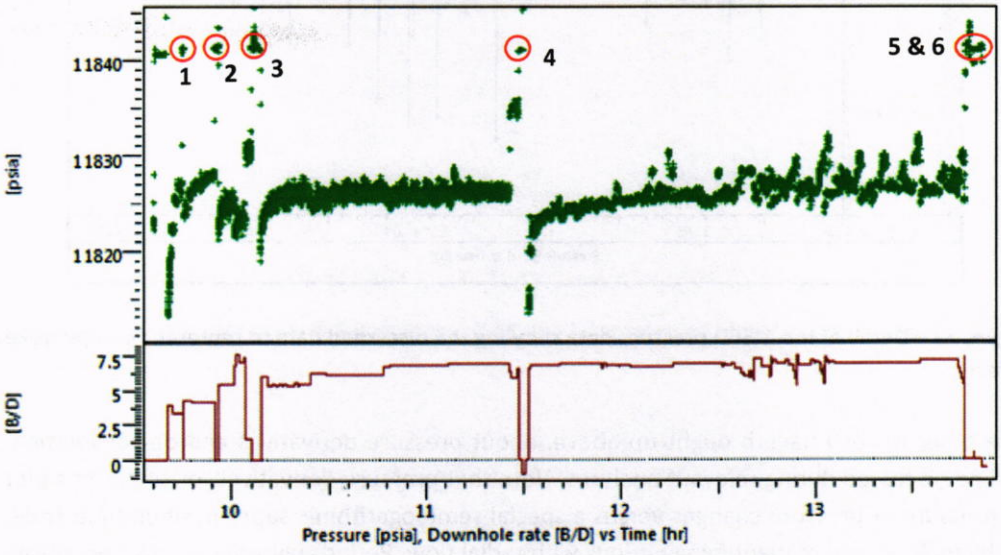

Figure 14 – Overview of the complete M56D data set with 6 buildups identified.

Although some of the derivatives at the bottom in Figure 15 do fall on a straight line with constant value, the general impression is that the derivatives display a downward trend closer to -1, and also a final upward trend. To determine if this is indeed the case, we have to take a closer look at the data, and this is best done in semi-log plots without any algorithm-based derivatives. For standard full-scale tests with higher rates, or wire-line tests in formations with lower mobility, the log-log plot normally provides the information we need to proceed along a standard workflow. However, for the Macondo data we have to be more careful.

Actually, the upward trend seen as a dominating feature towards the end of the semi-log derivatives in all of the log-log diagnostic plots of the Macondo MDT data is an artifact of gauge resolution and my direct use of recorded data. I am using recorded data directly since using smoothing on these data sets is unreliable given the scatter and limited number of data points from each buildup. The reason gauge resolution causes the derivatives to increase is that the superposition time axis compresses the data more and more with elapsed time since shut-in, and the minimal observable pressure change in these data sets is 0.01 psi. Avoiding increasing derivatives is therefore not possible, or at least highly unlikely,

during the buildups. Note that without pressure change the derivative will be zero, and not shown in a log-plot. If the change is negative and the absolute value displayed, then the problem will just be exaggerated.

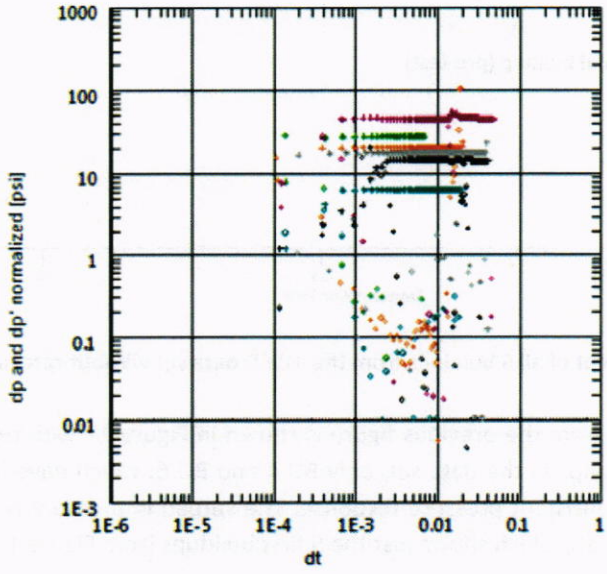

Figure 15 – Log-log diagnostic plot of all 6 buildups from the M56D data set normalized by rate.

Figure 16 shows a semi-log plot of all 6 buildups from the M56D data set without rate normalization. The "superposition" time scale used here accounts for rate changes prior to shut-ins (buildups). The horizontal shift in the data from the final buildup (i.e., the pre-test) is caused by a much lower rate prior to this buildup compared to the others.

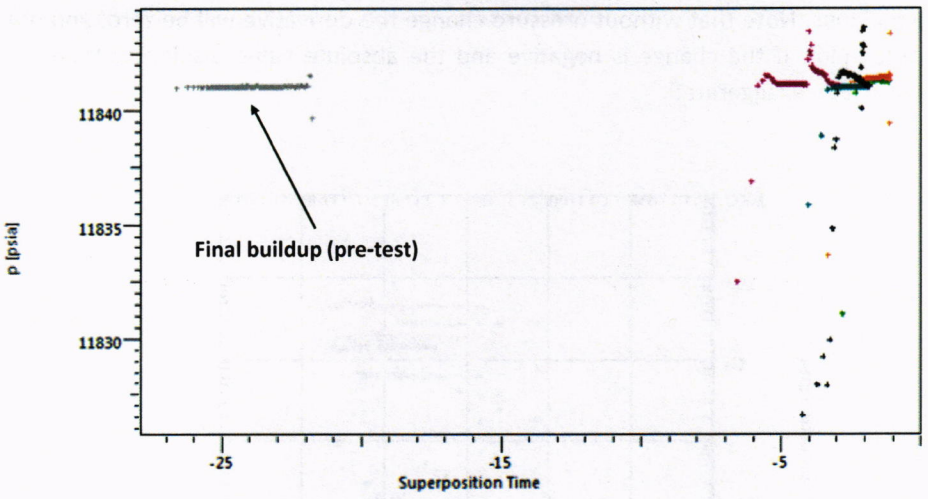

Figure 16 – Semi-log plot of all 6 buildups from the M56D data set without rate normalization.

A detail of the data from the previous figure is shown in Figure 17 with restricted pressure range. Of the 6 buildups in the data set, only BU 4 and BU 6, which have been identified in Figure 17, show a consistent pressure response. The spread in pressure response is further highlighted in Figure 18, which shows just the 5 first buildups from Figure 17.

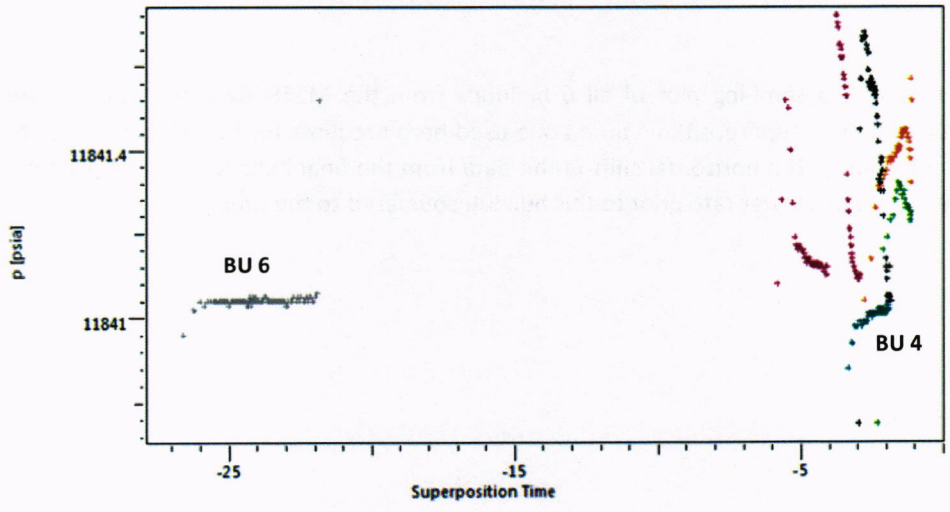

Figure 17 – Semi-log plot of all 6 buildups with a restricted pressure range.

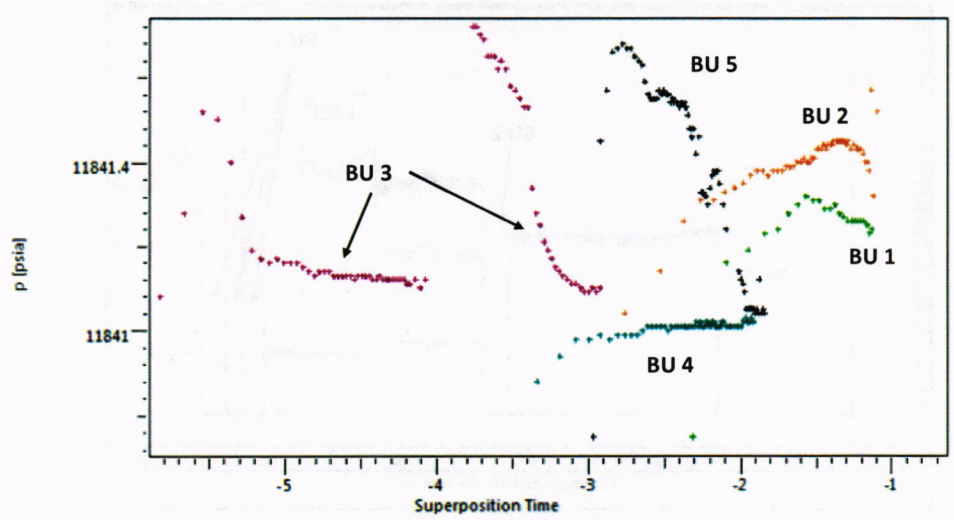

Figure 18 – Semi-log plot of the first 5 buildups with the same a restricted pressure range.

With reference to the data shown above we need to determine if the fact that only 2 out of 6 agree is caused by a random, and hence unreliable, tool response, or if there is a reason behind the results. To this end we need to look closer at the pump sequences. Note, however, that the data fall into two main categories: With "hump" in early data (BUs 3 and 5), and without "hump" (BUs 1, 2, 4 and 6).

From Figure 19 it is seen that only the guard pump was used prior to BU 1 and BU 2, and also that the sample pump was used between BU 2 and BU 3 along with the guard pump. Moreover, only the sample pump was operated for some time prior to BU 3, but the guard pump was also run briefly just before shut-in. During BU 3 there are also some pump activities recorded in the data, with at least the first period adversely affecting the BU 3 data in Figure 18 (the split). Actually, the initial hump in the BU 3 data has roughly the same duration as the short period with both pumps running prior to shut-in.

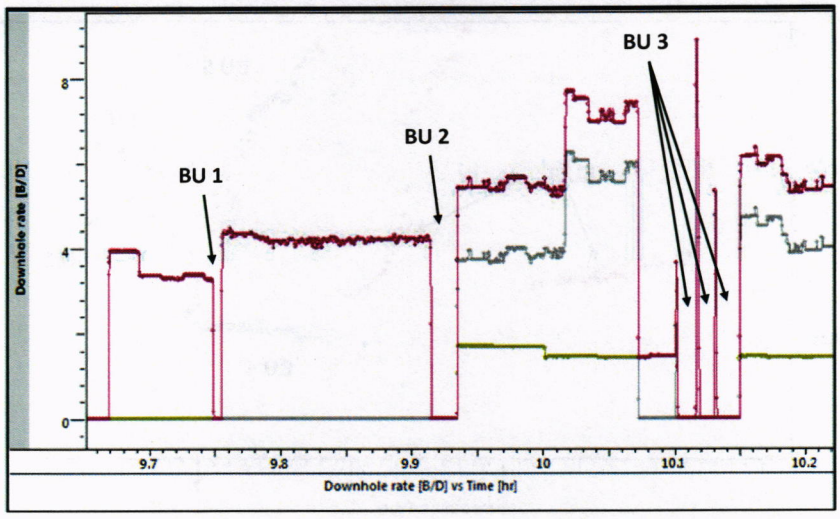

Figure 19 – Recorded pump rates from the start of the M56D data set through BU 3.

Figure 20 shows recorded rates leading up to BU 4. For this buildup, similar to BUs 1 and 2, only the guard pump is running for some time prior to shut-in. During the full length of the shut-in period, a period with injection is evident in the pressure data. I have made no attempt to use the injection and pressure falloff data in analyses, but a limited injection rate has been used in the rate history.

For BU 5, at the end of the M56D data set, it follows from Figure 10 that both pumps were operated at least for a period prior to BU 5. This buildup is therefore similar to BU 3, although the period with dual-pump flow was much shorter prior to BU 3.

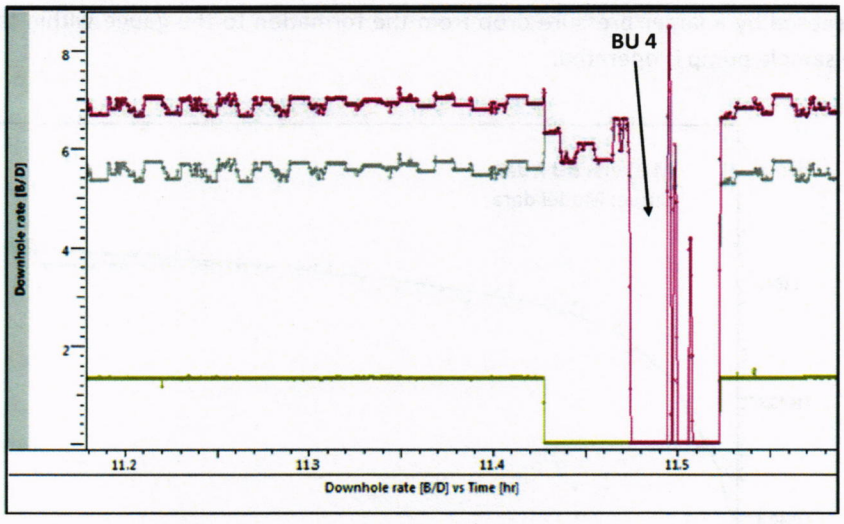

Figure 20 – Recorded pump rates from the M56D data set leading up to BU 4.

The natural conclusion from the observations above is that the pressure humps in BU 3 and 5 are caused by the two independent pumps being operated prior to shut-in, most likely from some form of pressure differentials after shut-in. Moreover, the deviating behavior seen in the BU 1 and 2 data is most likely caused by mud loss from the drilling operation. Poor data from early buildups is quite normal. Ending up with just 2 out of 6 buildups with a reliable pressure response from the M56D data set is therefore not surprising, and no cause for alarm.

Whether or not BU 4 and 6 can be used to determine the permeability of the M56D sand unit is still to be shown, with gauge resolution being the main problem.

6.3. Analyses of the M56D Data with Permeability 500 md

A semi-log match of data from BU 4 based on a single-probe model with horizontal permeability 500 md, vertical permeability 50 md, probe diameter 2 inches, skin value -0.12 and "wellbore" storage 6E-6 bbl/psi is shown in Figure 21. The analysis is based directly on recorded data without smoothing and use of modified data. An attempted log-log match of the same data is shown in Figure 22. The derivatives of the model data and of the BU 4 data are quite different. This is natural in view of the information one can possibly extract from the raw data in Figure 21.

A match of BU 4 data in the form of a history plot including a period with both pumps operating is shown in Figure 23. From this plot we see that even though the total rates are not much different, the drawdown is much larger when the sample pump is running. This

must be caused by a larger pressure drop from the formation to the gauge within the tool when the sample pump is operated.

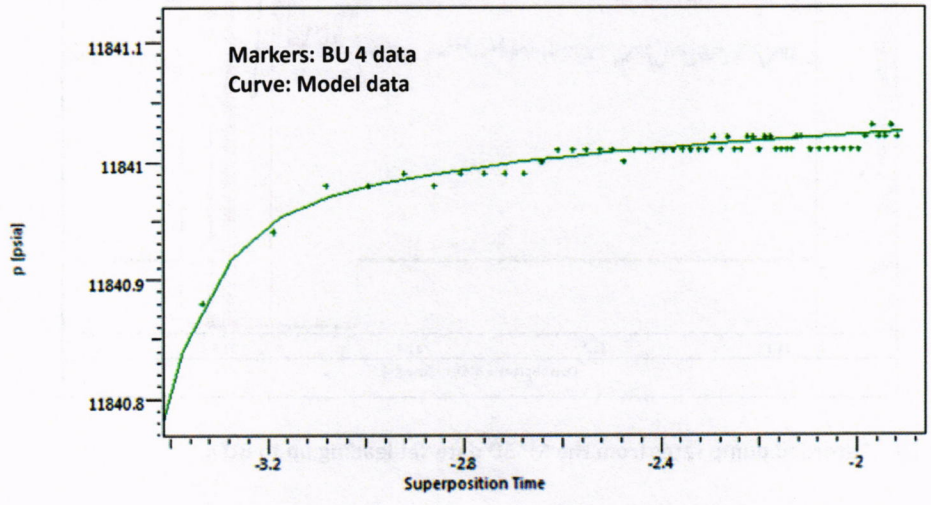

Figure 21 – Semi-log match of the data from BU 4 based on a single-probe model with horizontal permeability 500 md and vertical permeability 50 md.

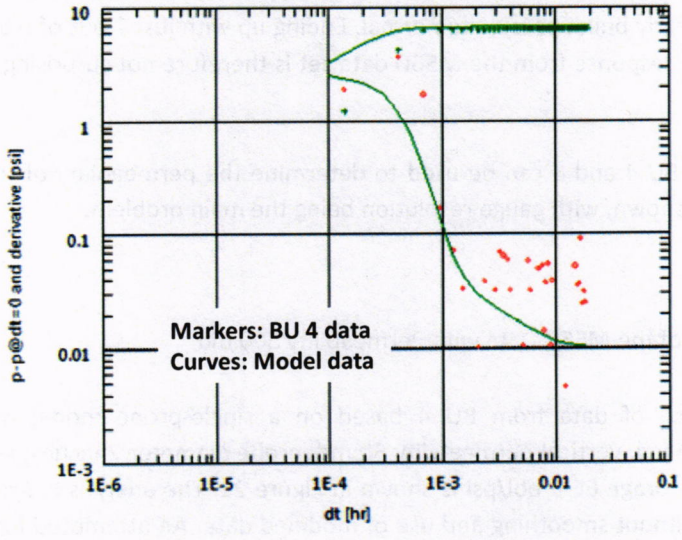

Figure 22 – Attempted log-log match of the BU 4 data from the previous figure.

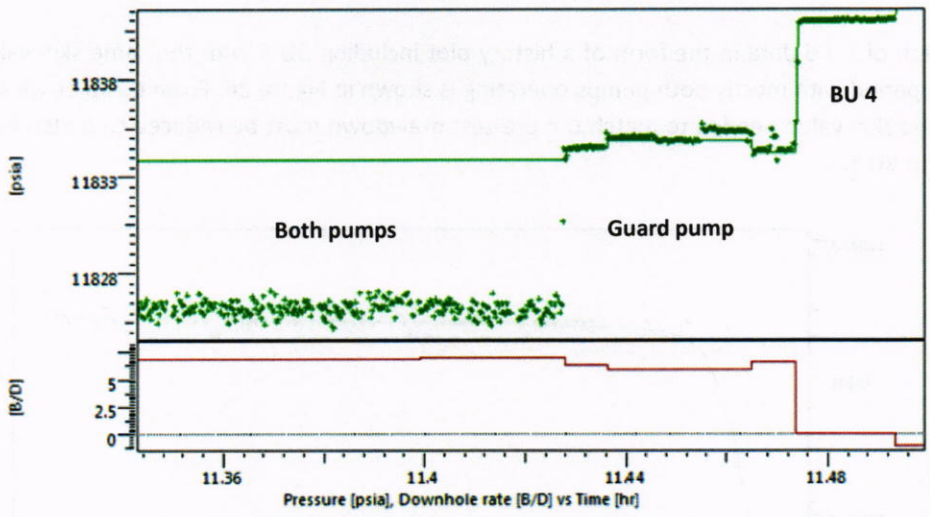

Figure 23 – History plot showing a match of BU 4 and periods with both dual and single-pump operations.

In the analysis above, and in other similar analyses, I have used a probe diameter of 2 inches as a reference value, with the actual value modified by the factor exp(-skin). For the case above the effective probe diameter derived from the analysis is therefore 2.3 inches. A modification is also added based on the k_V/k_H ratio, since the permeability contrast will affect the flow pattern near the probe opening. The importance of these ideas is that the actual condition in the formation near the probe opening is unknown, with the effective probe diameter obtained from the analysis indicating whether or not the connection is good or bad. A positive skin value will not have a direct impact on properties determined from an analysis, but a large negative value can imply that the results are invalid (probe diameter too large to seal within the wellbore), and hence that better properties must be used to match the data.

The "wellbore" storage parameter used in all data sets accounts for compressibility effects of fluids within the tool between the formation and the pump(s). Unfortunately, the effect of tool storage, which cannot be ignored, tends to disturb early data where a spherical-flow response should be observed. A steep drop in semi-log derivatives prior to the onset of radial can therefore be caused by precisely this effect.

A semi-log match of data from BU 6 based on the same single-probe model used for BU 4, but with a change in skin value to 0.77, corresponding to effective diameter of 0.93 inches, and storage to 2E-6 bbl/psi, is shown in Figure 24. The analysis is again based directly on recorded data without smoothing and use of modified data. An attempted log-log match of the same data is shown in Figure 25. Similar to BU 4, the derivatives of the model data and of the BU 6 data are quite different. This is again natural in view of the information one can possibly extract from the raw data in Figure 24.

A match of BU 6 data in the form of a history plot including BU 5 with the same skin value and a period with mostly both pumps operating is shown in Figure 26. From this plot we see that the skin value needed to match the pre-test drawdown must be reduced to match flow prior to BU 5.

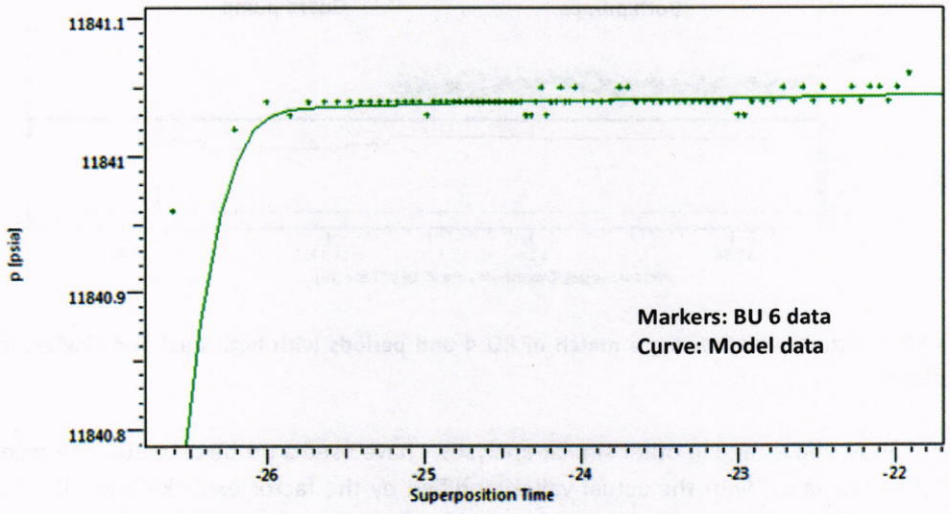

Figure 24 – Semi-log match of the data from BU 6 based on the same single-probe model with k_H = 500 md used for the BU 4 data with modified skin value.

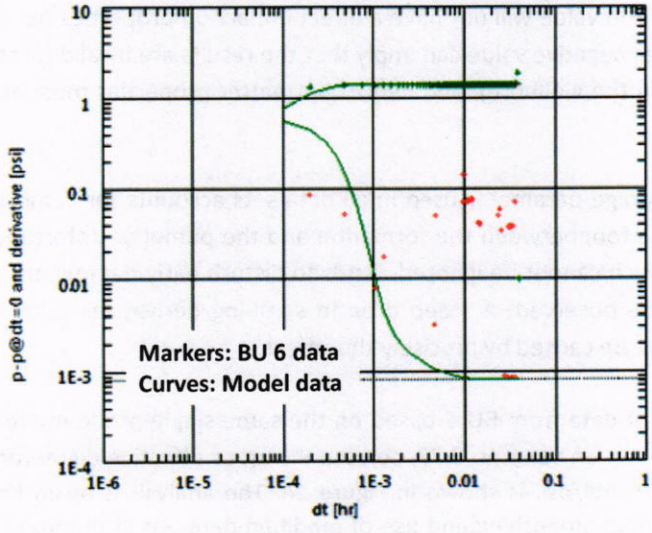

Figure 25 – Attempted log-log match of the BU 6 data from the previous figure.

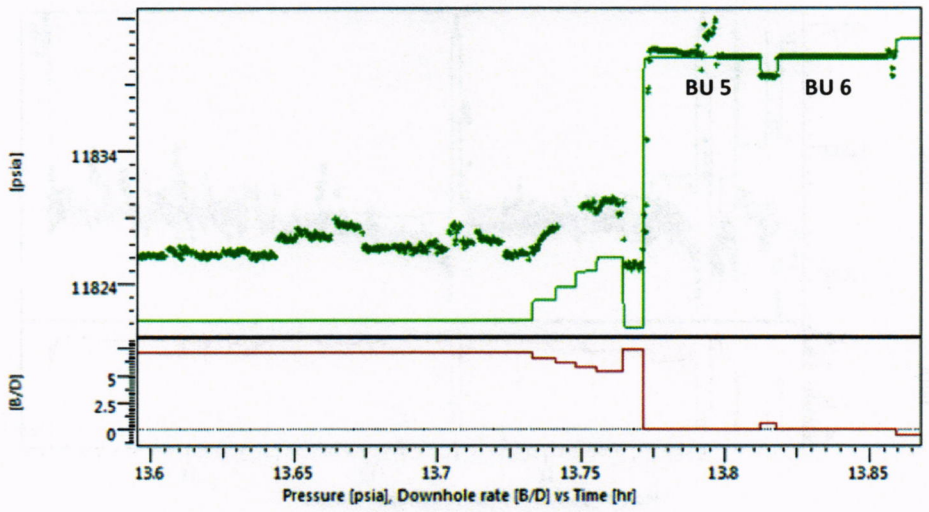

Figure 26 – History plot showing a match of BU 6 along with BU 5 and some flow data leading up to these buildups (BU 6 model).

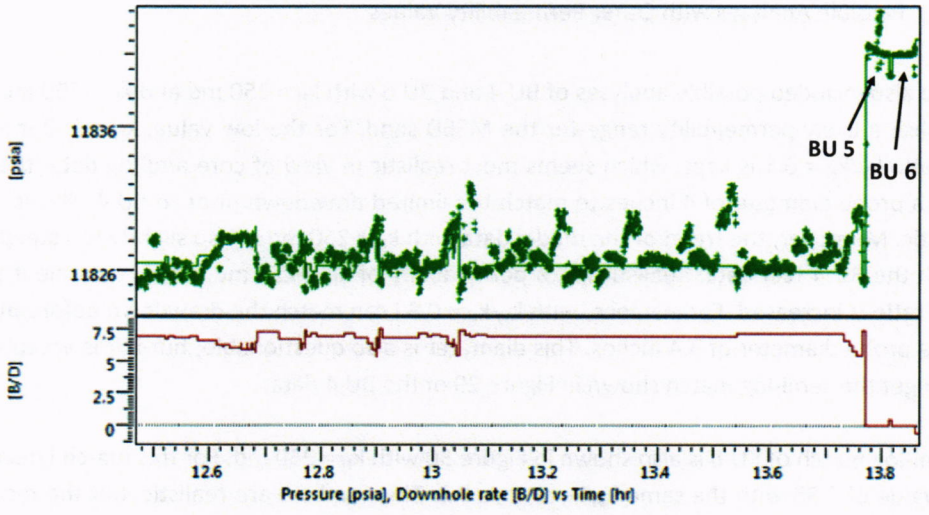

Figure 27 – History plot showing a match of BU 5 and BU 6 with skin value reduced to S = 0.52 to flow prior to BU 5.

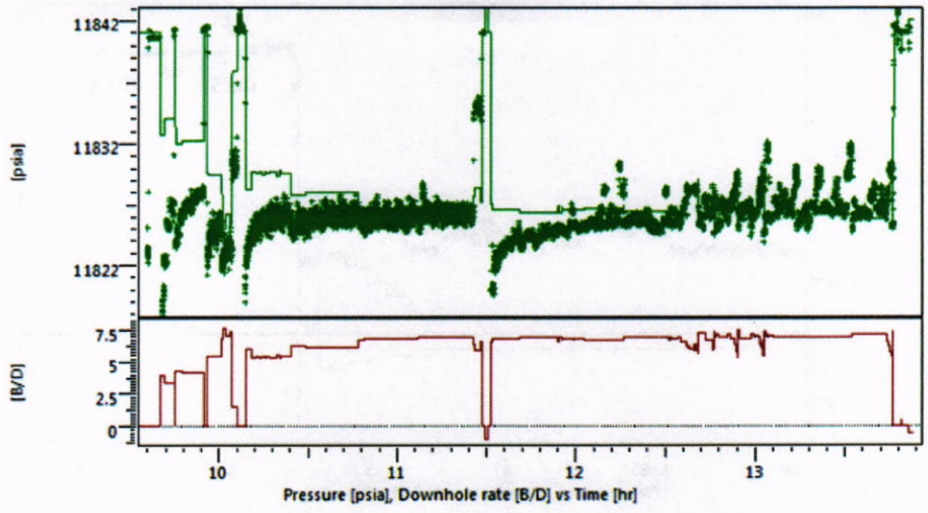

Figure 28 – Match of the entire M56D data with the BU 5 model (i.e., skin value).

6.4. Possible Analyses with Other Permeability Values

I have also included possible analyses of BU 4 and BU 6 with k_H = 250 md and k_H = 750 md to establish a likely permeability range for the M56D sand. For the low value, k_H = 250 md, if the ratio k_V/k_H = 0.1 is kept, which seems most realistic in view of core and log data, then I need a probe diameter of 4 inches to match the limited drawdown prior to BU 4. This is not realistic. Moreover, the trend of the model data with k_H = 250 md is also slightly too steep to match the BU 4 test data. Realistically, a permeability of k_H = 250 md is only possible if the k_V/k_H ratio is increased. For instance, with k_V/k_H = 0.3 I can match the drawdown before BU 4 with a probe diameter of 3.4 inches. This diameter is also questionable, but if it is accepted, then I get the semi-log match shown in Figure 29 of the BU 4 data.

A semi-log match of BU 6 is also shown in Figure 30 with k_H = 250 md. For this match I need a skin value of 0.35 with the same k_V/k_H ratio is 0.3. The numbers are realistic, but the model data slightly too steep in the match in Figure 30.

I have also included a semi-log match of BU 4 in Figure 31 with k_H = 750 md and k_V/k_H = 0.1. For this match I need to use a skin value of 0.22. A similar analysis is shown in Figure 32 for BU 6 with the same properties and skin 0.77. The skin values are realistic, but the trends are a little too shallow, indicated 750 md to be too high for the M56D sand.

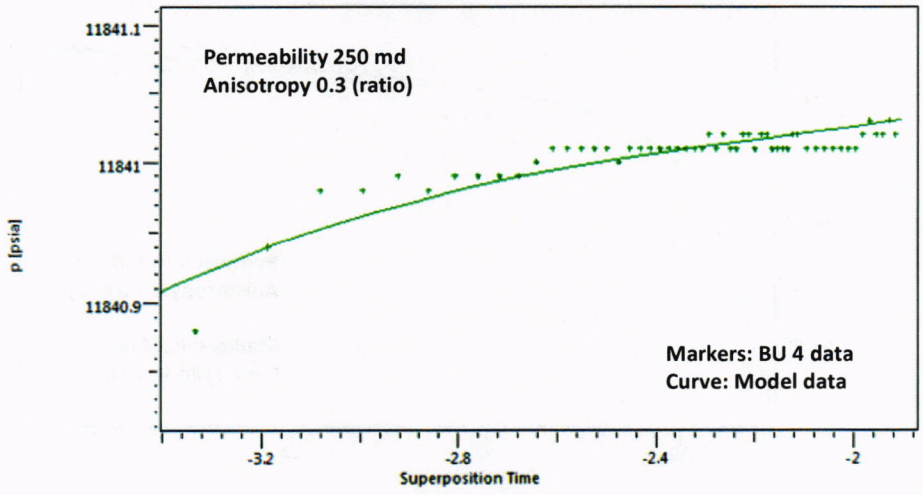

Figure 29 – Semi-log match of the data from BU 4 with k_H = 250 md and k_V/k_H = 0.3.

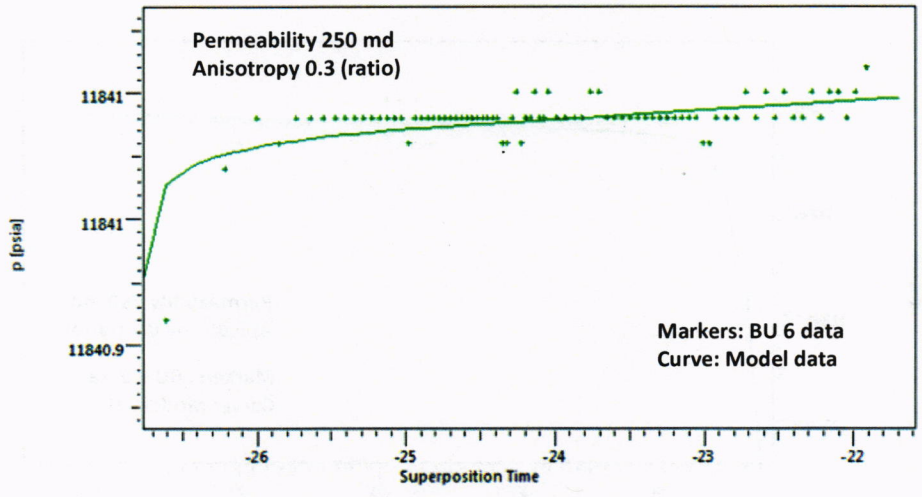

Figure 30 – Semi-log match of the data from BU 6 with k_H = 250 md and k_V/k_H = 0.3.

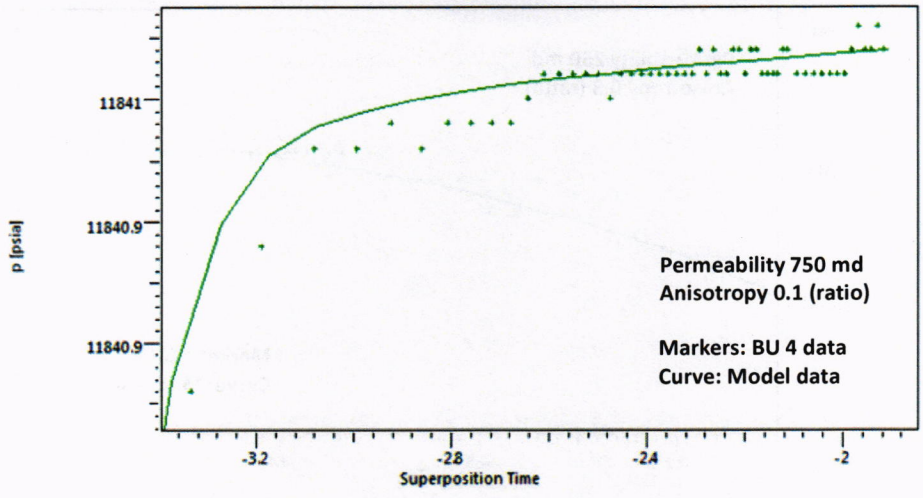

Figure 31 – Semi-log match of the data from BU 4 with permeability 750 md and k_V/k_H = 0.1.

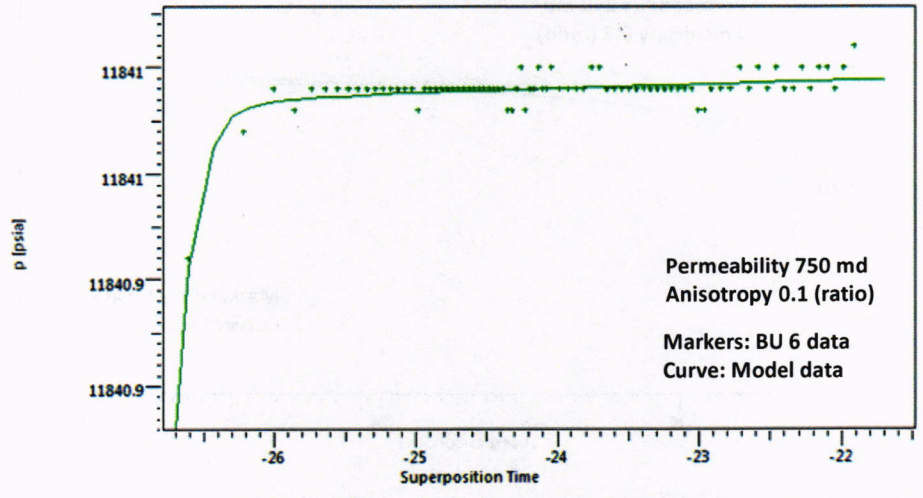

Figure 32 – Semi-log match of the data from BU 6 with permeability 750 md and k_V/k_H = 0.1.

7. DETAILED ANALYSES OF DATA FROM THE UPPER M56E SAND

7.1. Rate Data from Upper M56E

Figure 33 shows an overview of recorded total and individual rates from the guard and sample pumps in the Upper M56E data set. At this station the sample pump was started after roughly 22 minutes. Moreover, in Figure 34, which shows the last part of pump data, the sample pump is seen to be throttled back prior to the last shut-ins.

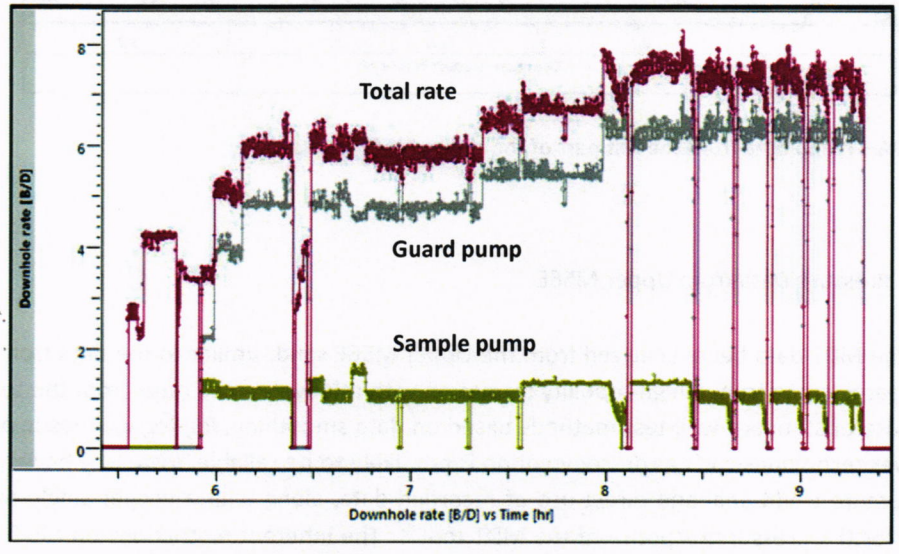

Figure 33 – Overview of the rate data from Upper M56E, with split between the guard and sample pumps shown.

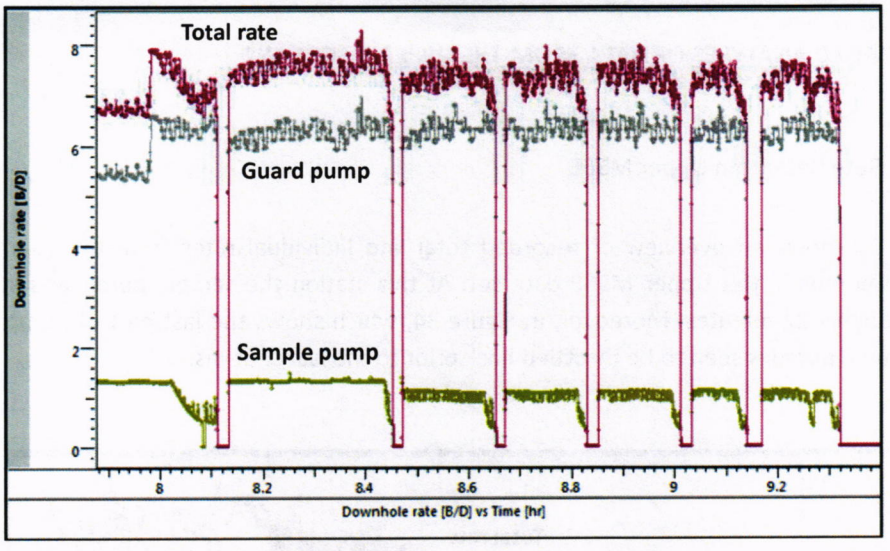

Figure 34 – Pump data from the last part of the Upper M56E data set.

7.2. Pressure Data from Upper M56E

Since the MDT data being analyzed from the Upper M56E sand, similar to the data from the M56D sand, come from a high-mobility formation with relatively small rates from the tool, a direct use of standard well-test methods based on data smoothing, log-log diagnostic plots, or newer techniques such as de-convolution is not likely to be reliable. Instead, I have again used a more traditional and direct use of recorded data, along with a proper single-probe model for the pressure response of the MDT tool.[22] The inherent restrictions on MDT data were described for the M56D data set above, where the approach I have used to remove pressure outliers from pump effects to get a cleaner data set for display purposes was also discussed and illustrated. For shut-in periods I have used recorded data directly without any filtering or smoothing of derivatives.

Figure 35 shows an overview of the complete Upper M56E data set following removal of pressure outliers from pump effects, with 12 buildups identified.

---

[22] Larsen, L.: "Modeling and Analyzing Source and Interference Data From Packer-Probe and Multiprobe Tests," paper SPE 102698 presented at the SPE Annual Technical Conference and Exhibition, San Antonio, Texas, 24–27 September 2006.

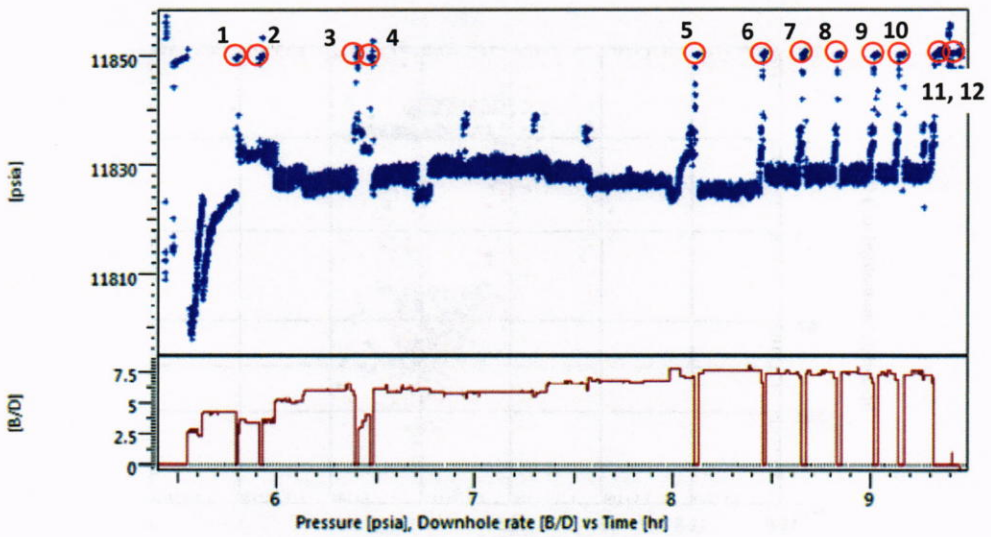

Figure 35 – Overview of the complete Upper M56E data set with 12 buildups identified.

In order to identify flow regimes, such as radial or spherical, in a given data set, the standard approach is to display buildup data in log-log diagnostic plots of pressure changes and semi-log derivatives. Figure 36 shows such data from all 6 buildups normalized with respect to rate to get a common late-time asymptote in derivatives (lower markers) if we have consistent data. In this plot, derivatives of radial-flow data should fall on a straight line with constant value, while derivatives of spherical-flow data should fall on a straight line with slope -1/2 (one square by two squares). With flow to a point, spherical flow is expected prior to radial flow – if radial flow is reached.

Although some of the derivatives at the bottom in Figure 36 do fall on a straight line with constant value, the general impression is that the derivatives display downward trend closer to -1, and also a final upward trend. To determine if this is indeed the case, we have to take a closer look at the data, and this is best done in semi-log plots without any algorithm-based derivatives. For standard full-scale tests with higher rates, or wire-line tests in formation with lower mobility, the log-log plot normally provides the information we need to proceed along a standard workflow. However, for the Macondo data we have to be more careful.

As was explained for the M56D data set, the upward trend seen as a dominating feature towards the end of the semi-log derivatives in all of the log-log diagnostic plots of the Macondo MDT data is just an artifact of gauge resolution. I have therefore not tried to use this behavior in any modeling and analysis effort.

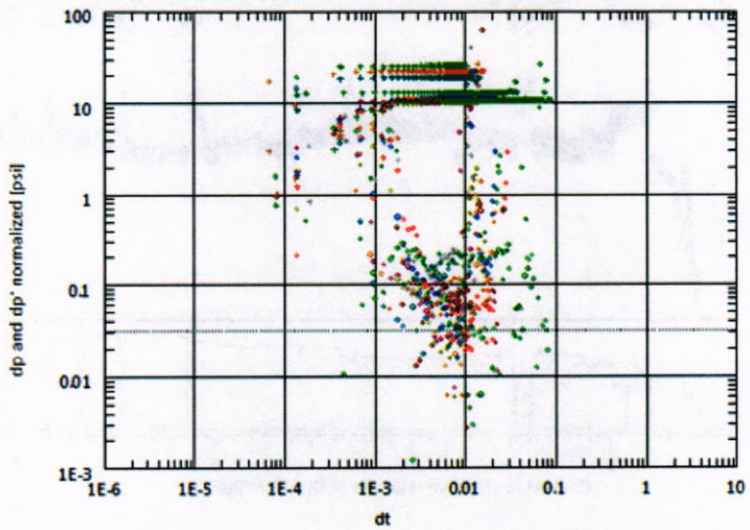

Figure 36 – Log-log diagnostic plot of all 12 buildups from the Upper M56E data set normalized by rate.

Figure 37 shows a semi-log plot of all 12 buildups from the Upper M56E data set without rate normalization. The "superposition" time scale used here accounts for rate changes prior buildups. The horizontal shift in the data from the final buildup (from the pre-test) is caused by a much lower rate prior to this buildup compared to the others.

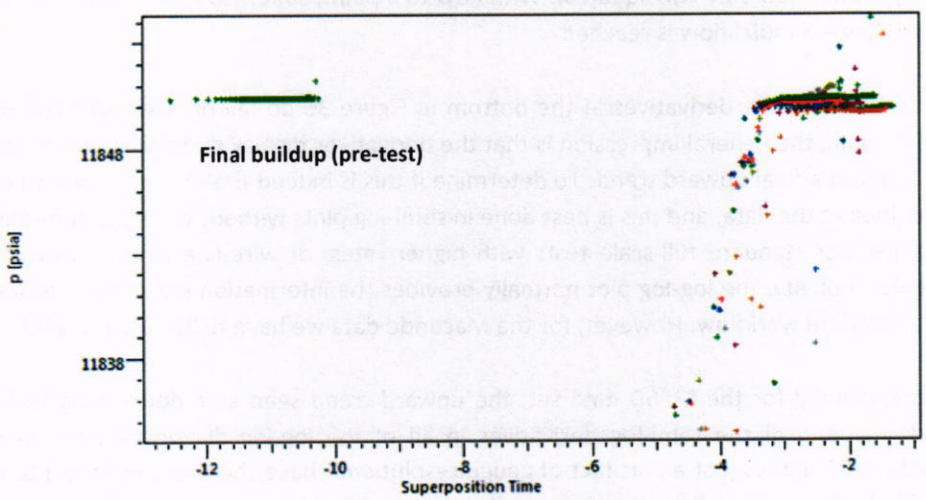

Figure 37 – Semi-log plot of all 12 buildups from the Upper M56E data set without rate normalization.

A detail of the data from the previous figure is shown in Figure 38 with restricted pressure range. It is not clear from this plot if there is a consistent subset of the 12 buildups. As a first impression it also appears that the pressure level of the first 11 buildups (the cluster on the right-hand of the plot) is lower than that from the last buildup (BU 12). Actually with higher rates for the first 11 buildups the slopes are steeper, and only a direct match with model data can be used to conclude if the pressure levels are indeed inconsistent. Note, however, that lower recorded pressures are possible with a heavier fluid between probe and a gauge higher in the MDT module (increased pressure drop).

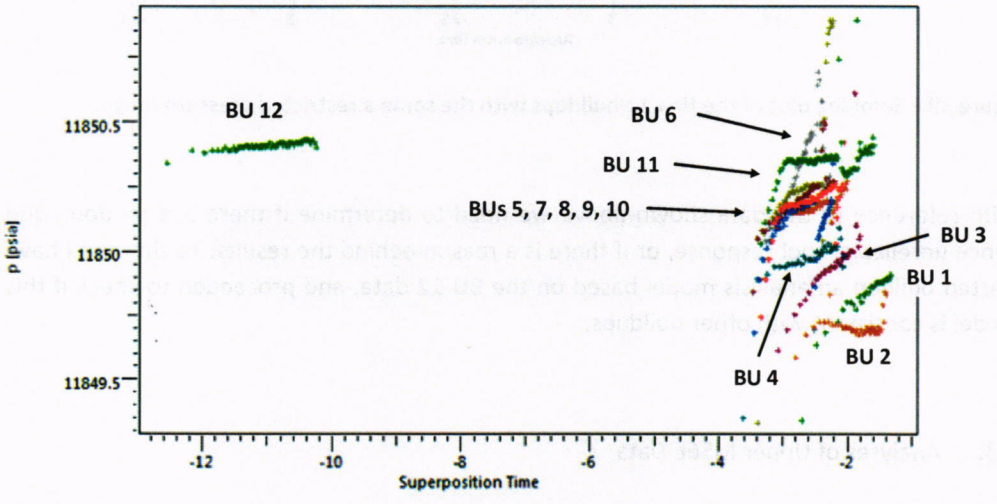

Figure 38 – Semi-log plot of all 12 buildups with a restricted pressure range.

Without directly identifying the various buildups, Figure 39 shows that most of them exhibit similar trends, but with vertical shifts that needs to be examined.

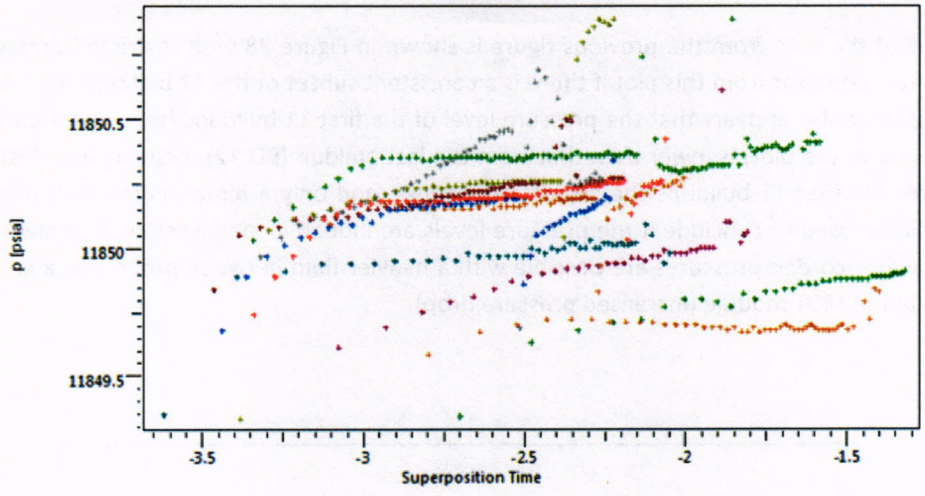

Figure 39 – Semi-log plot of the first 11 buildups with the same a restricted pressure range.

With reference to the data shown above we need to determine if there is a random, and hence unreliable, tool response, or if there is a reason behind the results. To this end I have started buildup an analysis model based on the BU 12 data, and proceeded to check if this model is consistent with other buildups.

7.3. Analyses of Upper M56E Data

A semi-log match of data from BU 12 based on a single-probe model with horizontal permeability 150 md, vertical permeability 15 md, and a reference probe diameter of 2 inches is shown in Figure 40. In this analysis, which is based directly on recorded data without smoothing or use of modified data, I have used a skin value of -0.25 and a tool storage of 1E-6 bbl/psi. The skin value implies an effective probe diameter of 2.6 inches. An attempted log-log match of the same data is shown in Figure 36. The derivatives of the model data and of the BU 12 data are quite different. This is natural in view of the information one can possibly extract from the raw data in Figure 35.

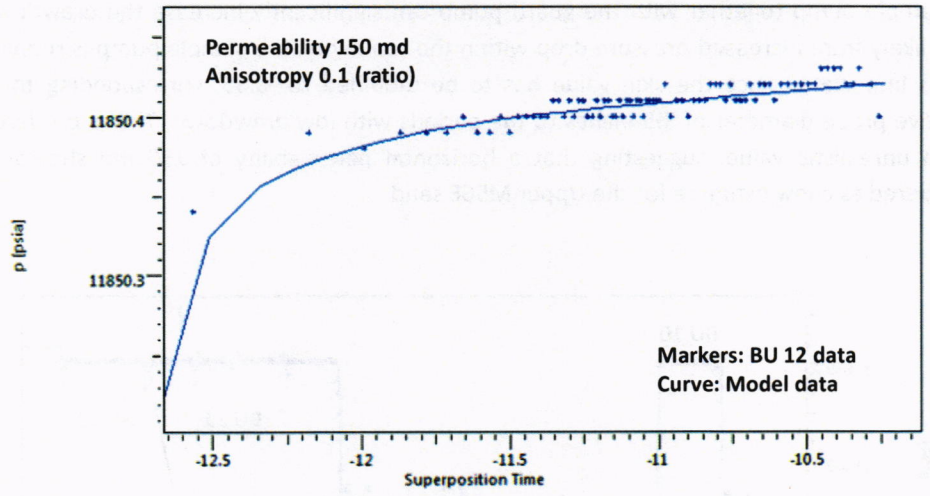

Figure 40 – Semi-log match of the data from BU 12 based on a single-probe model with horizontal permeability 150 md and vertical permeability 15 md.

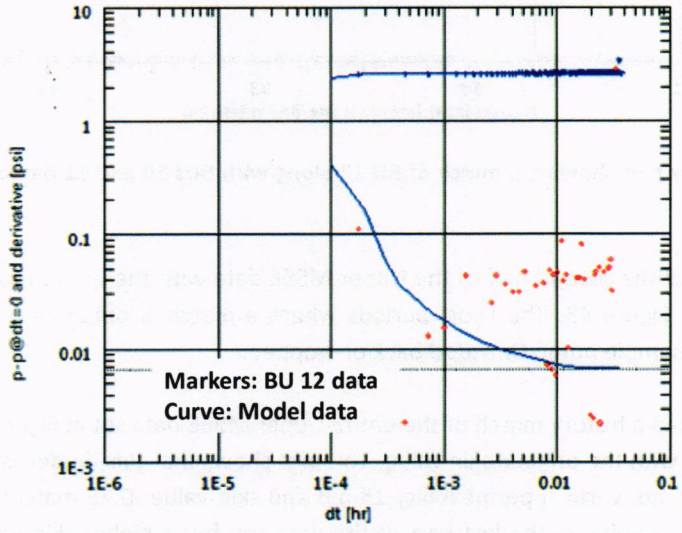

Figure 41 – Attempted log-log match of the BU 12 data from the previous figure.

I have also included a history plot in Figure 42 which shows a match based on the BU 12 model over a time span that also covers BUs 10 and 11. Note that both pumps were used over most of the flow periods, but 3 periods where the sample pump was throttled back is also evident in the pressure data (the half-domes). The latter point is important, because it follows that the drawdown is reduced significantly at low sample-pump rates even though the total rate does not change that much. As I pointed out for the M56D data set, operating

the sample pump together with the guard pump can significantly increase the drawdown, most likely from increased pressure drop within the tool when the sample pump is running. This is important, since the skin value has to be modified to -0.55, corresponding to an effective probe diameter of 3.5 inches to the periods with low drawdown. This is bordering on an unrealistic value, suggesting that a horizontal permeability of 150 md should be considered as a low estimate for the Upper M56E sand.

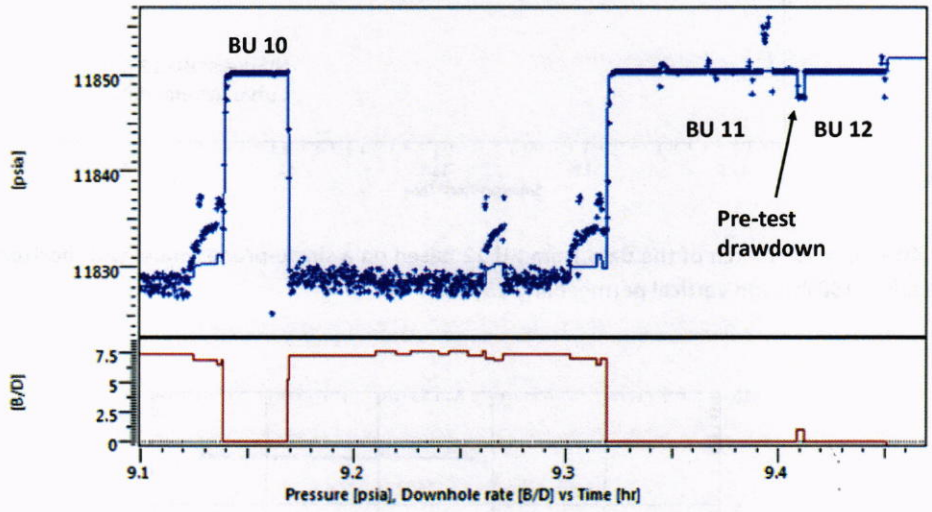

Figure 42 – History plot showing a match of BU 12 along with BUs 10 and 11 based on the BU 12 model.

A history match of the second half of the Upper M56E data with the BU 12 model and skin -0.55 is shown in Figure 43. The short periods where a match is obtained is precisely the periods with the sample pump throttled back or stopped.

I have also included a history match of the entire Upper M56E data set in Figure 44 based on the BU 12 model with the original skin value. This plot shows that this model, with horizontal permeability 150 md, vertical permeability 15 md and skin value -0.25 matches the periods with both pumps running in the last part of the data set, but a higher skin value (closer to zero or positive) is needed to match earlier data. Cleanup in the form of filtrate flow-back is the most likely reason for the reduction in drawdown relative to rate observed in the first part of the data. This is the normal response from such tests.

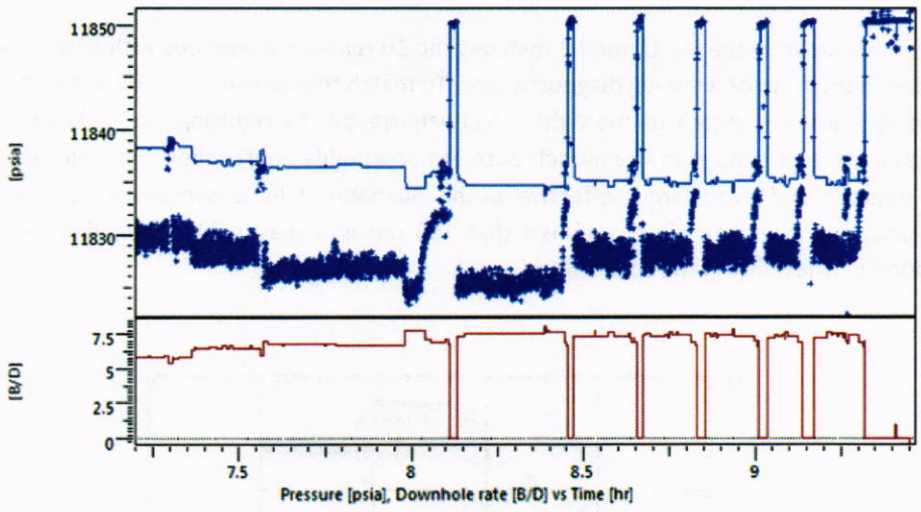

Figure 43 – History plot showing a match of short periods with only the guard-pump running, with increased probe diameter (modified skin value) used to match the data.

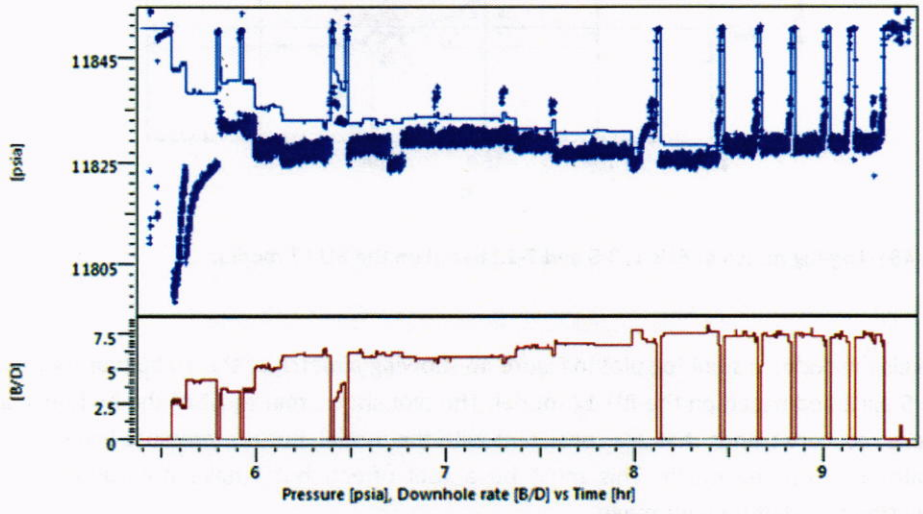

Figure 44 – The history match from the previous figure extended to the entire UPPER M56E data set.

By examining the data in Figure 38 in detail, I have concluded that BUs 2 and 6 cannot be used in analyses. BU 2 comes early, with problems therefore normal, while BU 6 appears to affected by operational disturbances, which are quite common considering that fluid sampling is normally the main objective from MDT runs.

Figure 45 shows how the BU 12 model matches the 10 remaining buildups with BUs 2 and 6 excluded in the form of a log-log diagnostic plot. To match the derivatives of data, the model derivatives must be shifted to the right. I can achieve this by reducing the k_V/k_H ratio or increasing the tool storage in the model. Both are acceptable approaches, but reducing the k_V/k_H requires and even larger effective probe diameter. I have considered this to be unrealistic, and have therefore assumed that 150 md is a reasonable lower limit of the horizontal permeability in the Upper M56E sand.

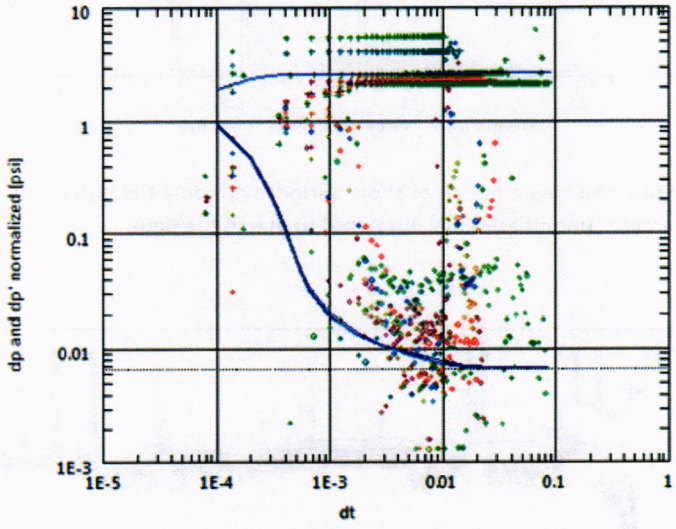

Figure 45 – Log-log match of BUs 1, 3-5 and 7-12 based on the BU 12 model.

I have also included a semi-log plot in Figure 46 showing a match of the 10 buildups with BUs 2 and 6 excluded based on the BU 12 model. The plot shows that most of the buildups have pressure recovery trends that are consistent with the model, but the pressure levels are too low, although not by much. This must be a tool effect, but I have not found a good explanation for what it might mean.

With the pressure levels from earlier buildups falling below that of the last buildup, using de-convolution to enhance the analysis of Upper M56E data is not a valid option.

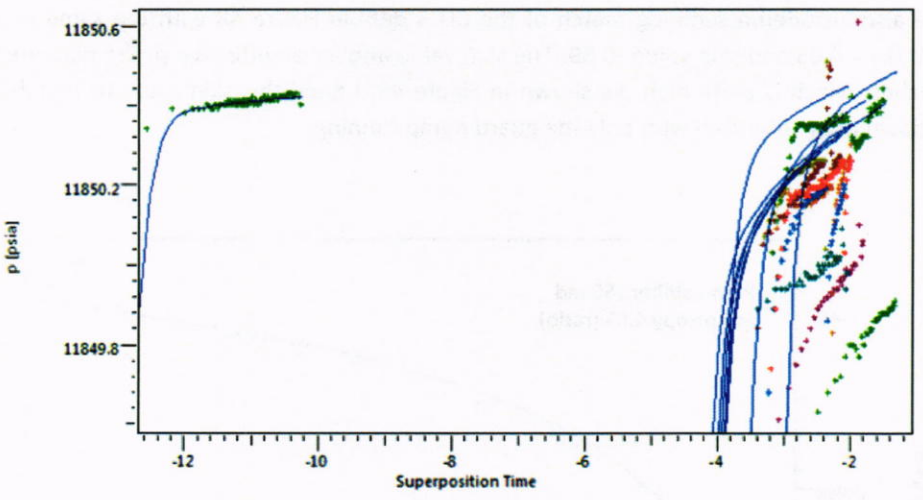

Figure 46 – Semi-log match of BUs 1, 3-5 and 7-12 based on the BU 12 model.

Although I have not shown this directly, the buildup trend from BU 1 is slightly steeper than that predicted by the BU 12 model. I have therefore reduced the k_V/k_H ratio 0.03 to match the BU 1 data with horizontal permeability 150 md. The resulting match with skin value 0.16 is shown in Figure 47. Reducing the k_V/k_H ratio to match early data might be questionable, but not unrealistic if considerable cleanup is achieved near the wellbore.

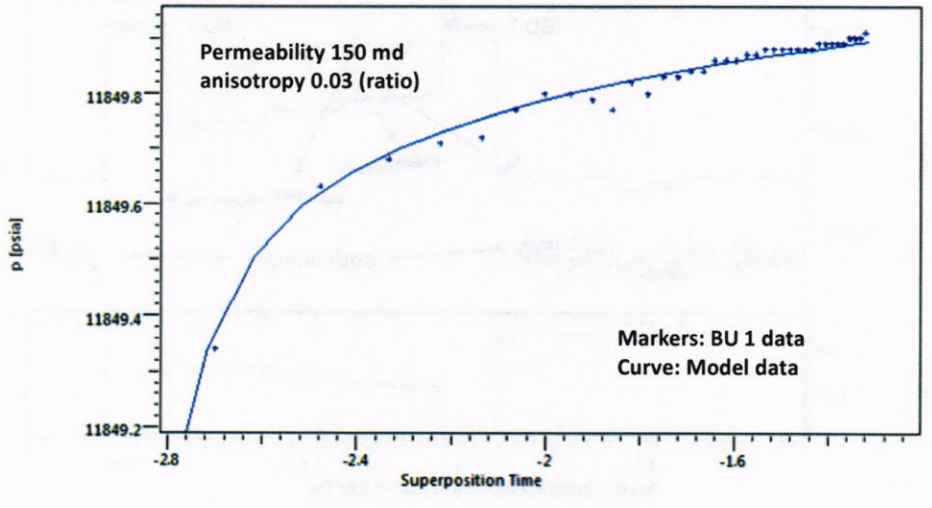

Figure 47 – Semi-log match of the data from BU 1 with k_H = 150 md and k_V/k_H = 0.03.

I have also included a semi-log match of the BU 3 data in Figure 48 with the same model with k_V/k_H = 0.03 and skin value -0.59. The skin value implies an effective probe diameter of 3.6 inches, which is quite high. As shown in Figure 49, I need this skin value to match the drawdown prior to shut-in with only the guard pump running.

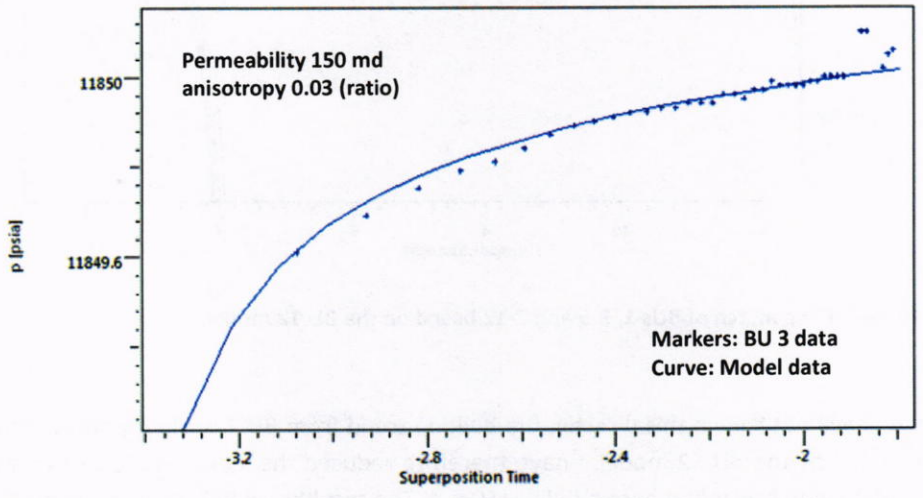

Figure 48 – Semi-log match of the data from BU 3 with k_H = 150 md and k_V/k_H = 0.03.

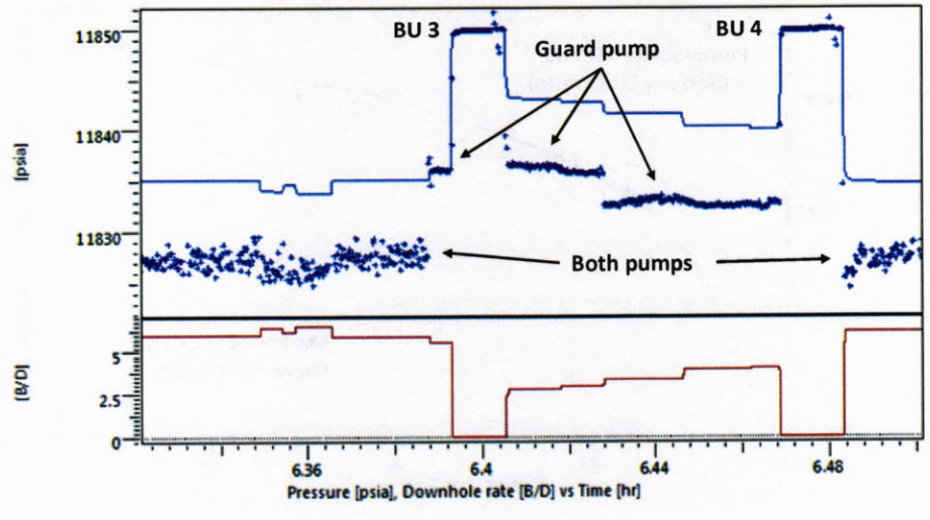

Figure 49 – History match of the data from BU 3 with k_H = 150 md, k_V/k_H = 0.03 and -0.59.

Although not shown in the report, I can also produce similar matches of several of the other buildups from the Upper M56E data set.

To get an indication of a possible permeability range from the Upper M56E sand I have also included an analysis of the BU 12 data with horizontal permeability 200 md. This is shown in the form of a semi-log plot in Figure 50. To achieve this match I have used a k_V/k_H ratio of 0.03 and a skin value of -0.23.

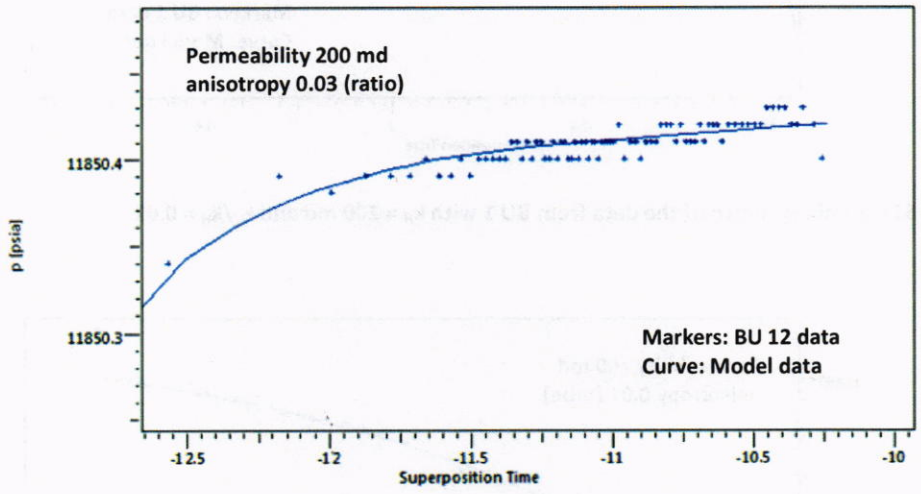

Figure 50 – Semi-log match of the data from BU 12 with k_H = 200 md and k_V/k_H = 0.03.

By following the approach used above, I can also match BU 1 and BU 3 data with the same model if I reduce the k_V/k_H ratio to 0.01. The first such match is shown in Figure 51, which is based on a skin value of 0.2.

In Figure 52 I show a similar analysis for BU 3 with skin value -0.55, corresponding to an effective probe diameter of 3.5 inches (a high value).

Both of these matches look acceptable, but the probe diameter does seem to be too high, or at least questionable.

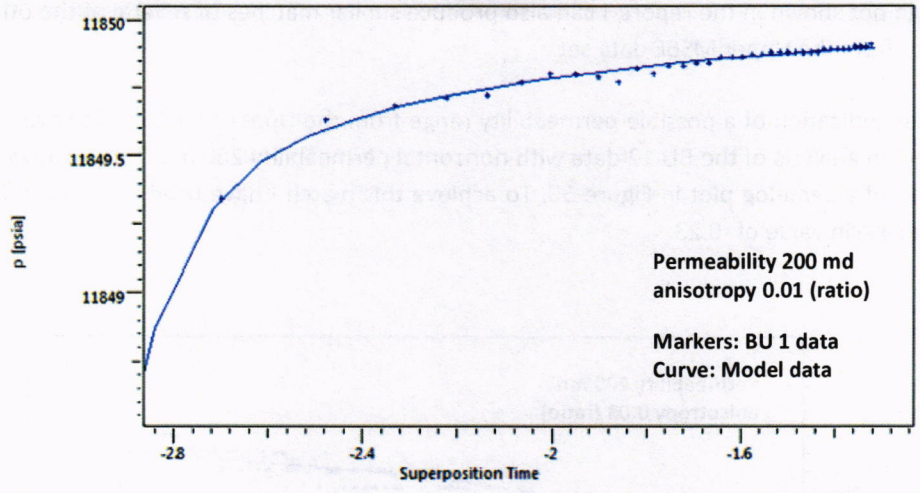

Figure 51 – Semi-log match of the data from BU 1 with k_H = 200 md and k_V/k_H = 0.01.

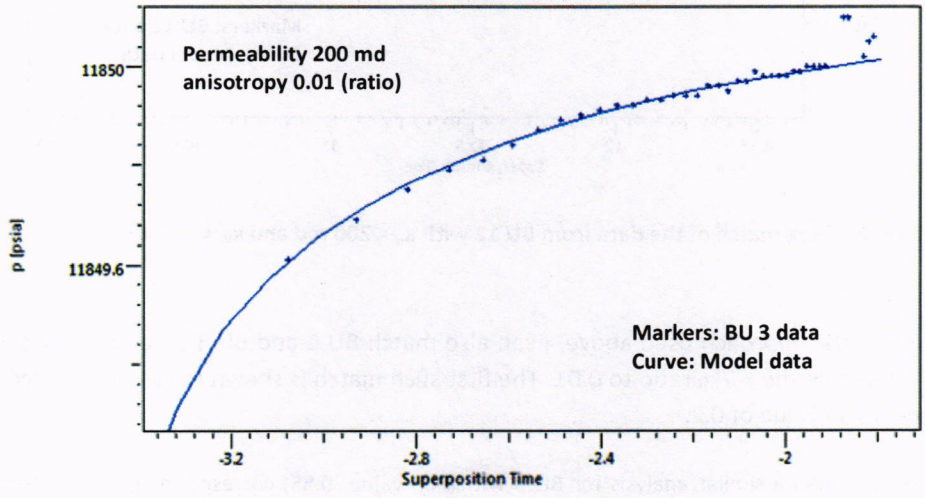

Figure 52 – Semi-log match of the data from BU 3 with k_H = 200 md and k_V/k_H = 0.01.

I have not included analyses with k_H = 250 md. The reason is that BU 12 requires a k_V/k_H ratio of 0.003 to match the trend of the bulk of the buildup data, but with this low ratio I cannot match early pressure data from BU 12 because the pressure recovery is too slow.

8. DETAILED ANALYSES OF DATA FROM THE LOWER M56E SAND

8.1. Rate Data from Lower M56E

Figure 53 shows an overview of recorded total and individual rates from the guard and sample pumps in the Lower M56E data set. At this station the sample pump was started after roughly 35 minutes. Similar to the other two data sets, the sample pump is throttled back prior to shut-in periods in the second half of the data. There are also some incorrect high rates in this data set, but these have just been ignored in analyses.

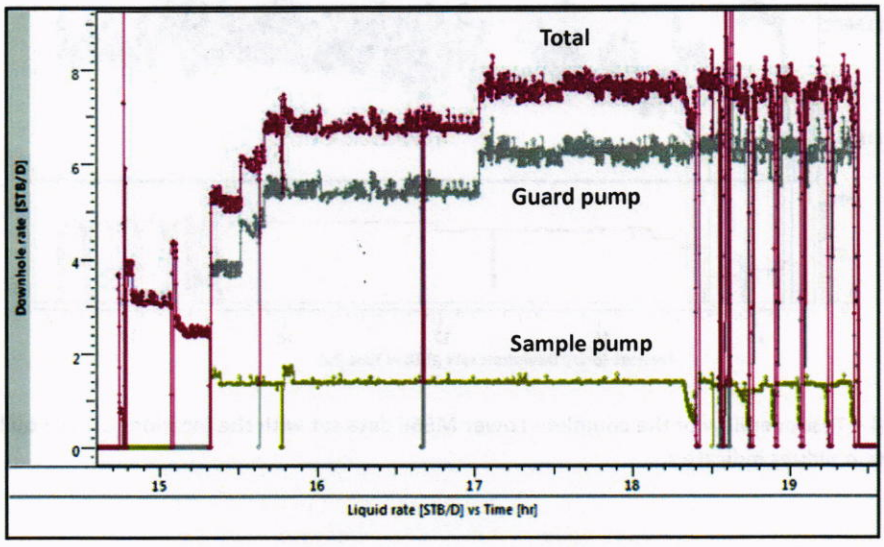

Figure 53 – Overview of the rate data from Lower M56E, with split between the guard and sample pumps shown.

8.2. Pressure Data from Lower M56E

The general statement about MDT data and the use of standard well-test methods based on data smoothing, log-log diagnostic plots, or newer techniques such as de-convolution, also apply to the data from the Lower M56E sand in the sense that one has to rely more directly on recorded data and the use of simple plots in analyses to avoid introducing false trends in the data. This only refers to shut-in periods. For periods with flow, the approach described for the M56D data set has been used for the Lower M56E data, with pressure outliers removed to get cleaner data in plots.

Figure 54 shows an overview of the complete Lower M56E data set with the location of 12 buildups indicated – 3 early in the data set and 9 towards the end. From this figure it is clear that the period leading up to the third buildup is strongly influenced by cleanup effects (filtrate flow back), while the last part with 9 quite periodic shut-ins taking place under relatively stable conditions, although with unstable rates. A detail of this period is shown in Figure 55. From this figure it appears that the buildup data are erratic and of questionable quality for use in analyses.

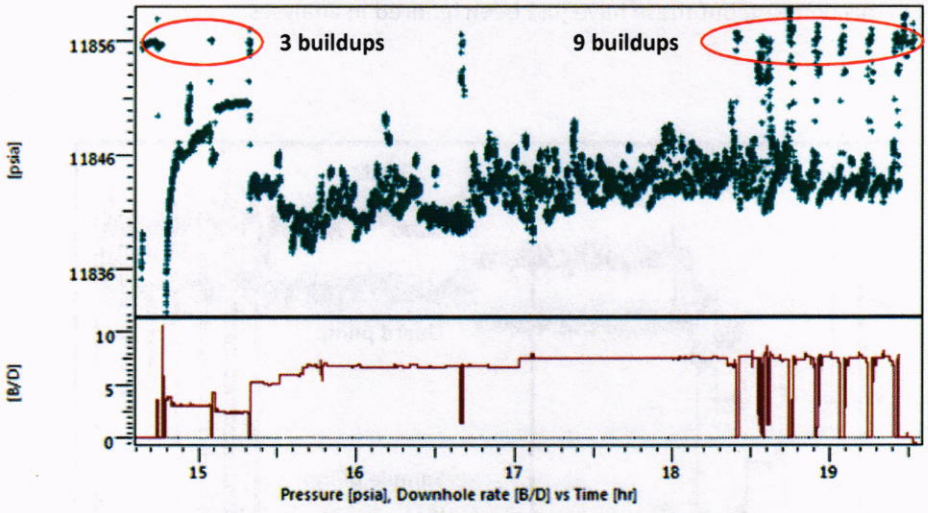

Figure 54 – Test overview of the complete Lower M56E data set with the locations 3 early buildups and 9 late buildups indicated.

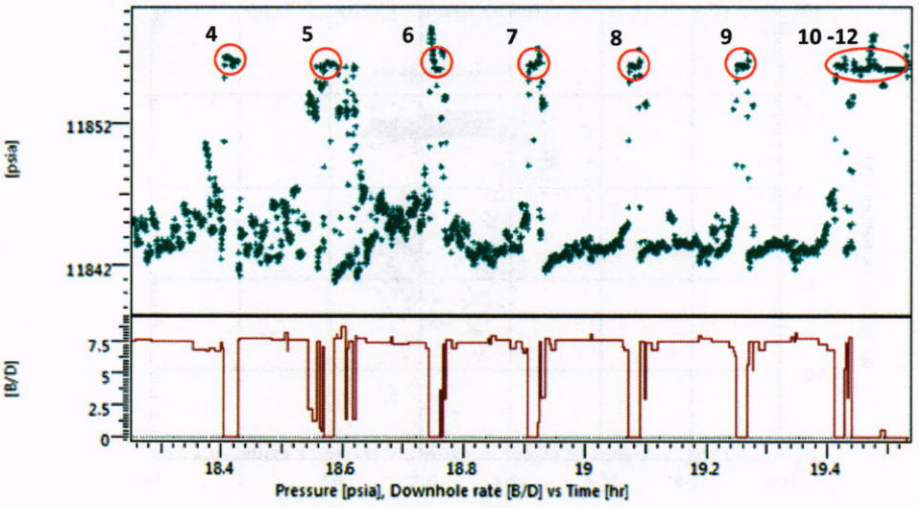

Figure 55 – Test overview covering the last part of the Lower M56E data with the location of the 9 late buildups indicated.

To get a first indication of the quality and information content in the 12 buildups from the Lower M56E data set I have followed standard procedure and set up the log-log diagnostic plot shown in Figure 56 with all 12 buildups included. The pattern seen in derivatives from the M56D and Upper M56E data sets is also repeated here, with a sharp down trend early and a steep uptrend at the end of the data. Although the downtrend is to some extent realistic and expected, the uptrend is not. As was explained for the M56D data set, the upward trend seen as a dominating feature towards the end of the semi-log derivatives in all of the log-log diagnostic plots of the Macondo MDT data is just an artifact of gauge resolution.

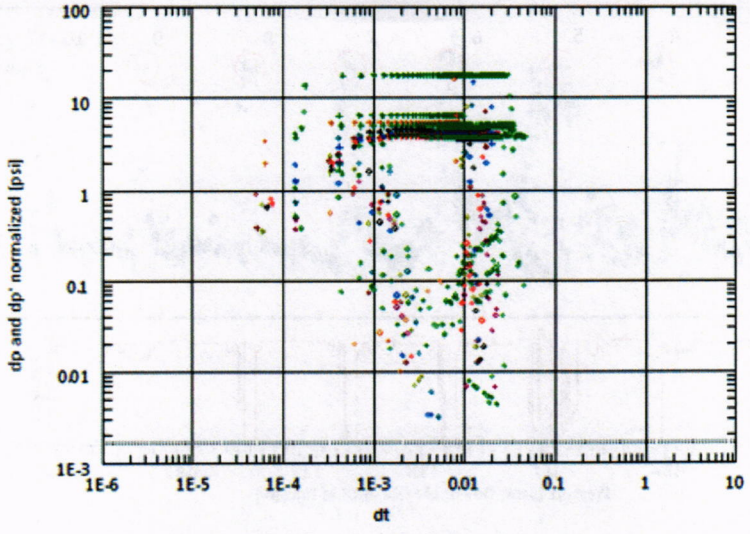

Figure 56 – Log-log diagnostic plot of all 12 buildups from the LOWER M56E data set normalized by rate.

In order to identify buildups that should be excluded from analyses I have used semi-log and linear plots to screen the data. Figure 57 shows a semi-log plot of all 12 buildups from the LOWER M56E data set without rate normalization. The "superposition" time scale is used to account for rate changes prior buildups. The horizontal shift in the data from the final buildup (from the pre-test) is caused by a much lower rate prior to this buildup compared to the others.

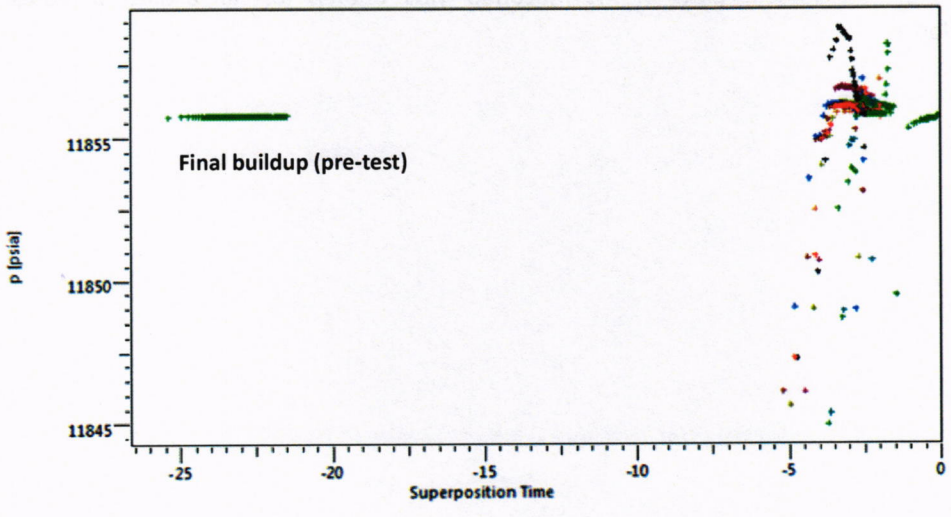

Figure 57 – Semi-log plot of all 12 buildups from the LOWER M56E data set without rate normalization.

A detail of the data from the previous figure is shown in Figure 58 with restricted pressure range and the first and last buildups identified (BUs 1 and 12). From this plot it is not possible to identify consistent buildups. From Figure 59, on the other hand, which is restricted to the first eleven buildups, it is possible to identify several buildups with declining pressure trend, and hence invalid data that cannot represent pressure buildup in the formation. These are BUs 2, 4, 5, 7, 8, 9 and 10. The reason must be tool effects or tool activities, either manual or automatic. Only the 5 remaining buildups, BUs 1, 3, 6, 11 and 12, can therefore possibly be used in analyses. BU 1, however, has a pressure level that is too low to represent an undisturbed formation response, leaving only 4 potential candidates: BUs 3, 6, 11 and 12.

Although BU 6 is highly disturbed, it has been used in some caparisons below. The reason is that it has a segment of data that overlays part of BU 11, and therefore appears to have some value.

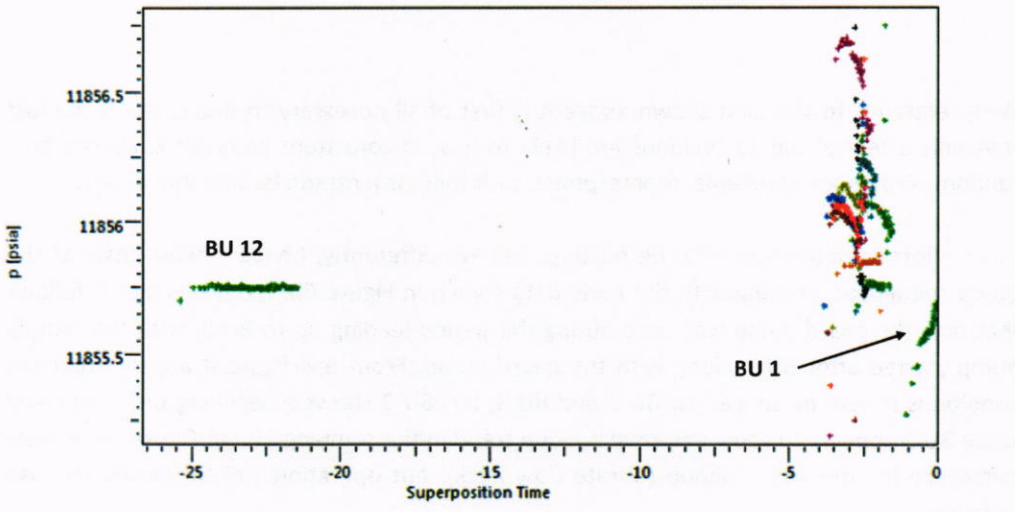

Figure 58 – Semi-log plot of all 12 buildups with a restricted pressure range.

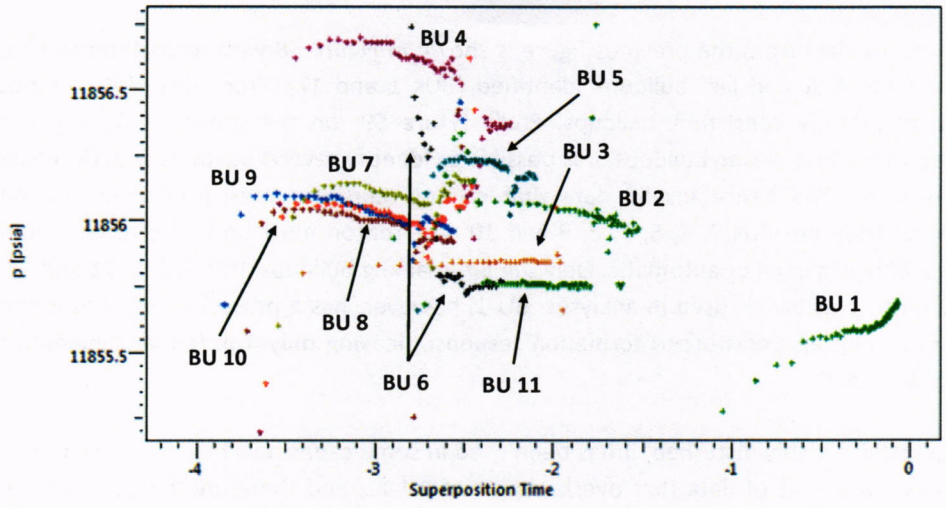

Figure 59 – Semi-log plot of the first 11 buildups with the same a restricted pressure range.

With reference to the data shown above it is first of all necessary to determine if the fact that only a few of the 12 buildups are likely to have a consistent behavior is caused by a random, and hence unreliable, tool response, or if there is a reason behind the results.

In an effort to determine why the buildups behave differently, I have looked closer at the pump sequences, starting with the early data shown in Figure 60. From this plot it follows that only the guard pump was used during the period leading up to BU 3, with the sample pump started after BU 3 along with the guard pump. From this figure it appears that the conditions should be similar for BU 2 and BU 3, but BU 2 shows a declining pressure trend while BU 3 appears to show a normal buildup trend in the semi-log plot in Figure 54. A likely difference is formation cleanup (filtrate flow back), but operational disturbances are also possible.

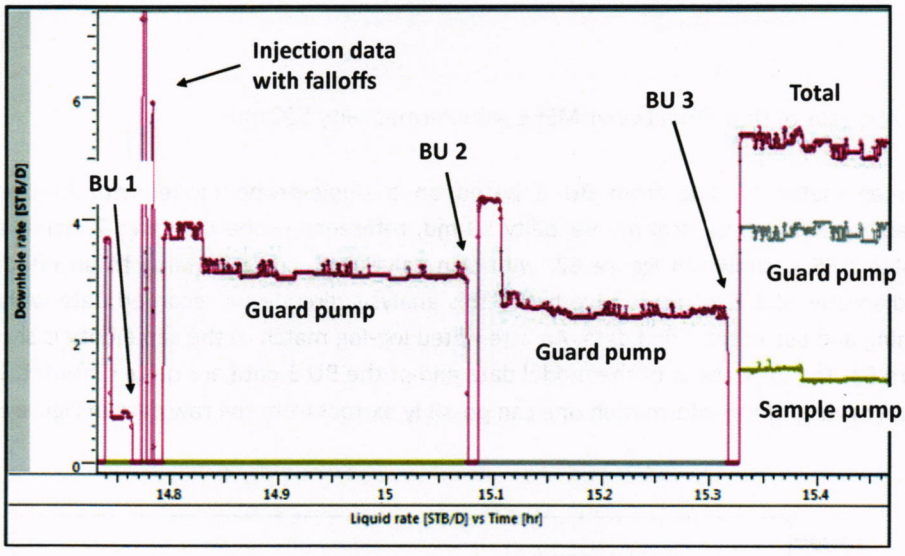

Figure 60 – Recorded pump rates from the start of the Lower M56E data set through BU 3.

For the remainder of the buildups it follows from Figure 61 that the sample pump was throttled back (for sampling purposes) to a low value prior to shut-in for BUs 4-10, while both pumps were running between BUs 10 and 11. Although BU 6 appears to have a similar pump sequence prior to shut-in as BUs 4, 5, 7-10, at least the end of this buildup appears to be valid for use in analyses.

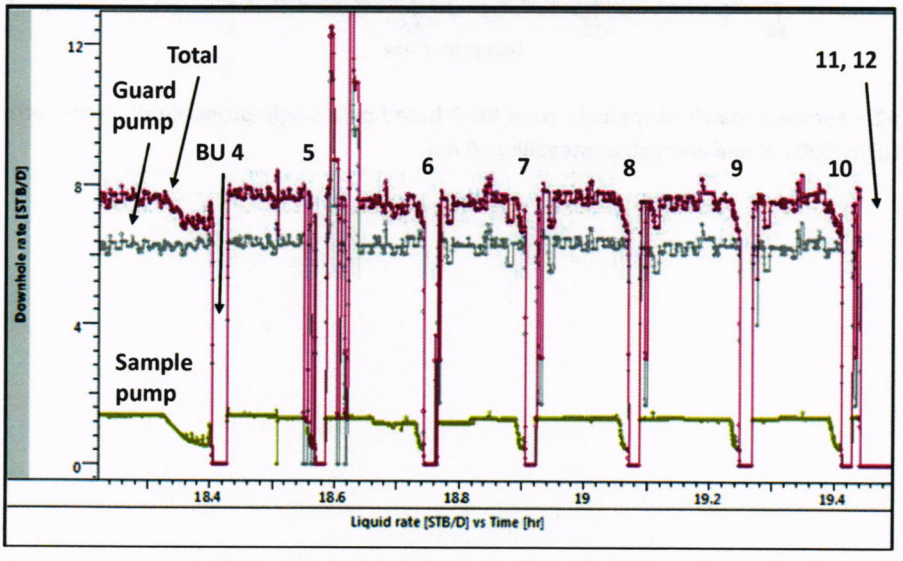

Figure 61 – Recorded pump rates from the last part of the Lower M56E data set.

8.3. Analyses of Data from Lower M56E with Permeability 500 md

A semi-log match of data from BU 3 based on a single-probe model with horizontal permeability 500 md, vertical permeability 50 md, reference probe diameter 2 inches and skin value 0.55 is shown in Figure 62, with skin value 0.55 corresponding to an effective probe diameter of 1.2 inches. I have based this analysis directly on recorded data without smoothing and use of modified data. An attempted log-log match of the same data is shown in Figure 63. The derivatives of the model data and of the BU 3 data are quite different. This is natural in view of the information one can possibly extract from the raw data in Figure 62.

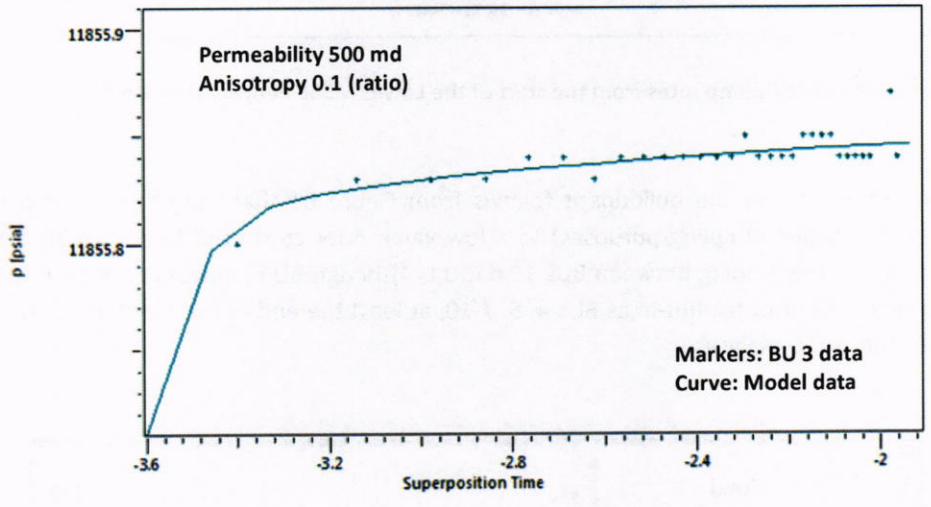

Figure 62 – Semi-log match of the data from BU 3 based on a single-probe model with horizontal permeability 500 md and vertical permeability 50 md.

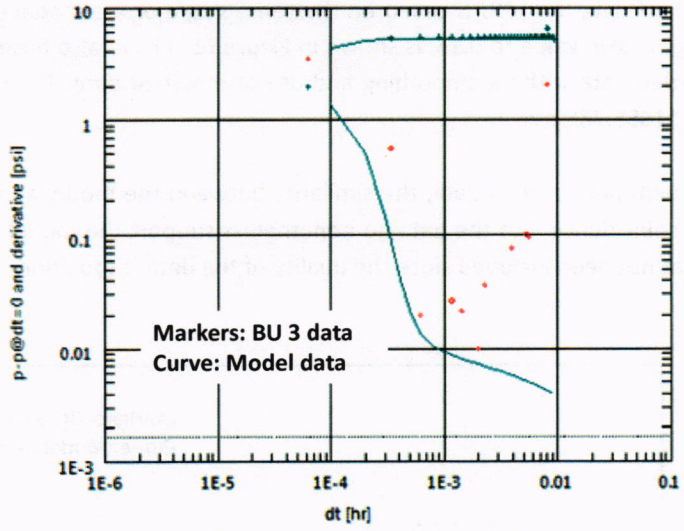

Figure 63 – Attempted log-log match of the BU 3 data from the previous figure.

The history plot in Figure 64 shows that the BU 3 model matches the entire flow period between BU 2 and BU 3, but not earlier data. The obvious reason is formation cleanup. This is indicated from the fact that the pressure is increasing (drawdown decreasing) while the rate is fairly stable.

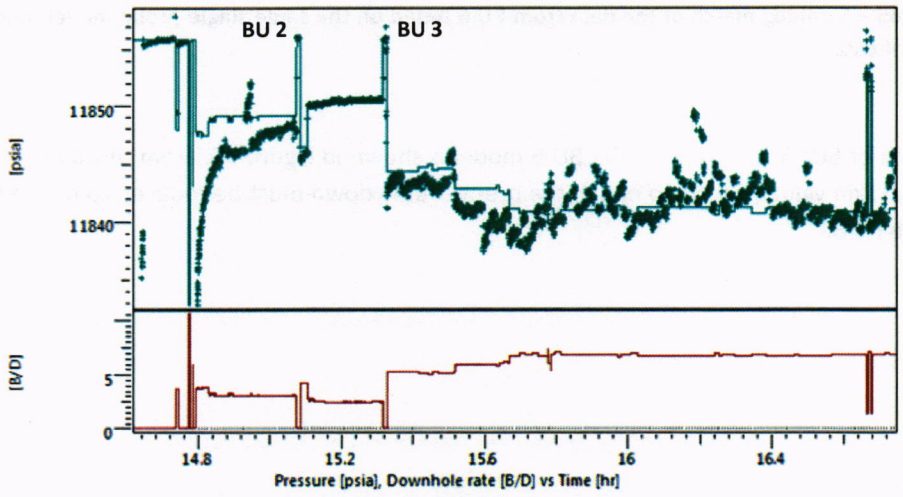

Figure 64 – History plot showing a match of BU 3 and periods with both dual, after BU 3, and single-pump operations, before BU 3.

A semi-log match of data from BU 6 based on the same single-probe model used for BU 3, but with a change in skin value to 0.13, is shown in Figure 65. I have also based this analysis directly on recorded data without smoothing and use of modified data. The initial pressure for this match is 11855.785 psia.

For this buildup with poor quality data, the similarity between the model and the recorded data might be a coincidence, but the data do nonetheless support the model. A log-log plot of this buildup has not been included since the quality of the data is too poor.

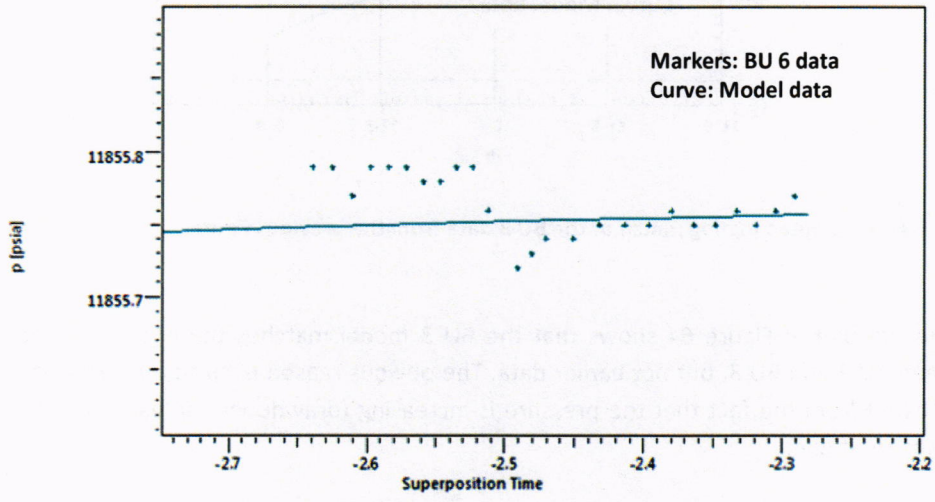

Figure 65 – Semi-log match of the data from BU 6 based on the same single-probe model used for the BU 4 data.

A match of BUs 5-12 based on the BU 6 model is shown in Figure 66. From this plot we see that the skin value needed to match the pre-test drawdown must be reduced to match flow prior to BU 5.

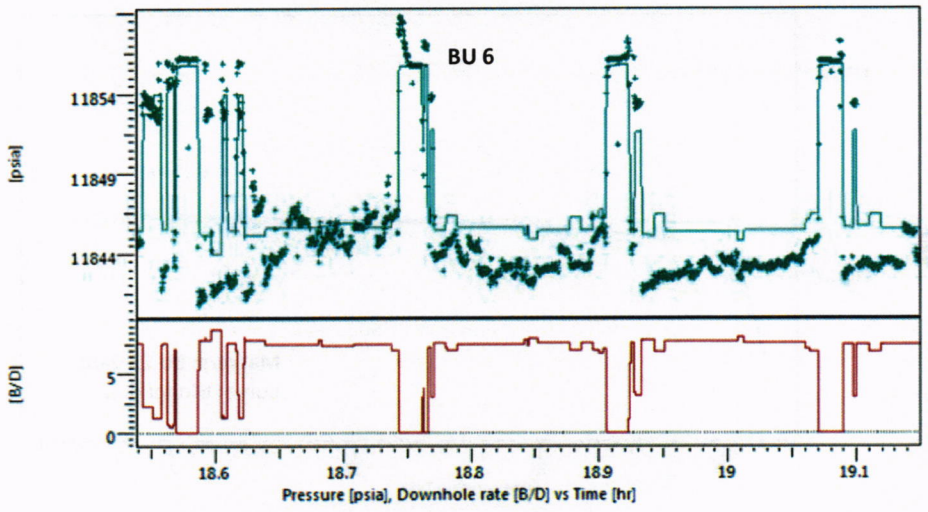

Figure 66 – History plot showing a match of BU 6 along with 7 of the other 8 buildups from the last group (BU 4 not included).

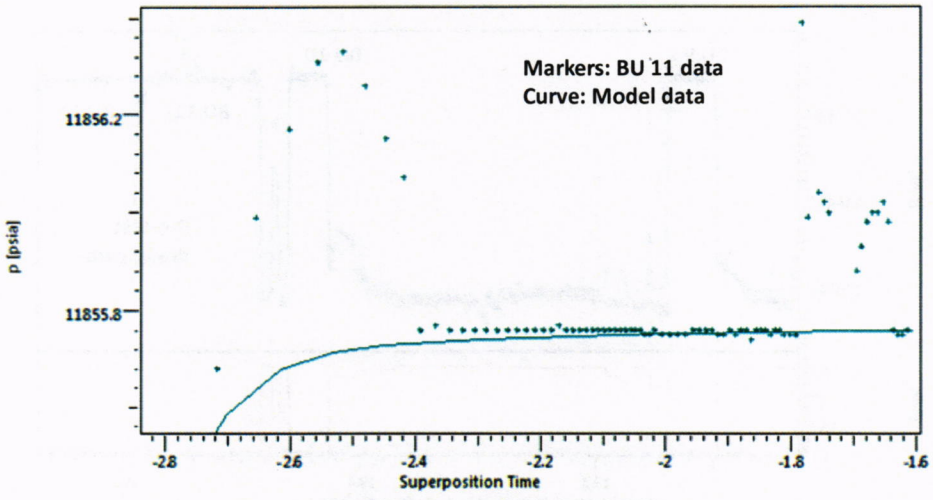

Figure 67 – Semi-log match of the data from BU 11 based on the same single-probe model used for the BU 3 and 6 data (restricted pressure range).

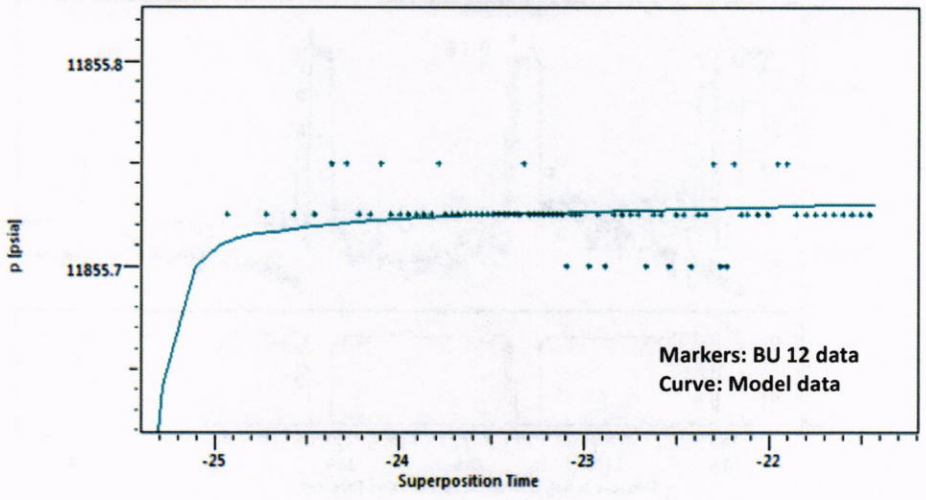

Figure 68 – Semi-log match of the data from BU 12 (pre-test) based on the same single-probe model used for the BU 3, 6 and 11.

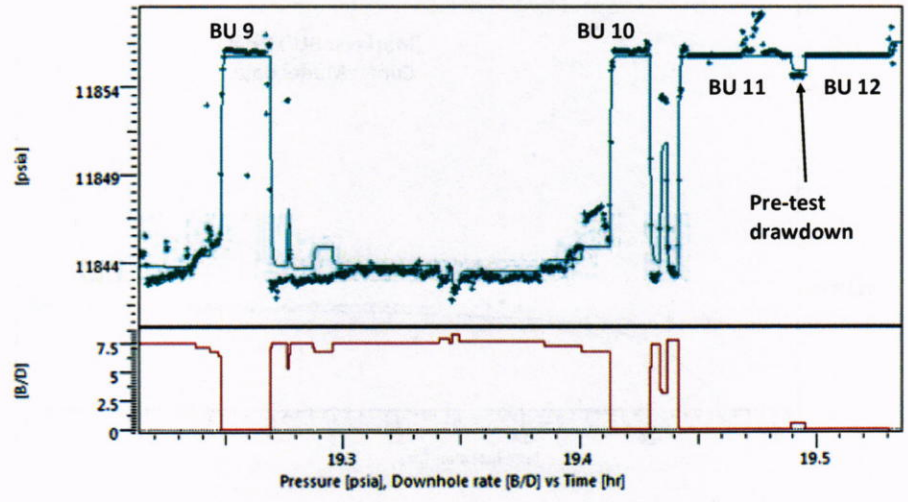

Figure 69 – History plot showing a match of BU 6 along with 7 others from the last group of buildups.

8.4. Possible Analyses of Lower M56E Data with Other Permeability Values

To get an indication of a possible permeability range from the Lower M56E sand I have also included analyses of BU 3 with horizontal permeability 250 md for a low value and 750 md for a high value. This is shown in the form of a semi-log plot in Figure 70 for the case with permeability 250 md and an isotropic formation (k_V/k_H = 1) with skin value 0.38. With a low k_V/k_H ratio, which is more realistic, the pressure recovery would be too slow, and hence indicate that a permeability of 250 md for this sand is too low.

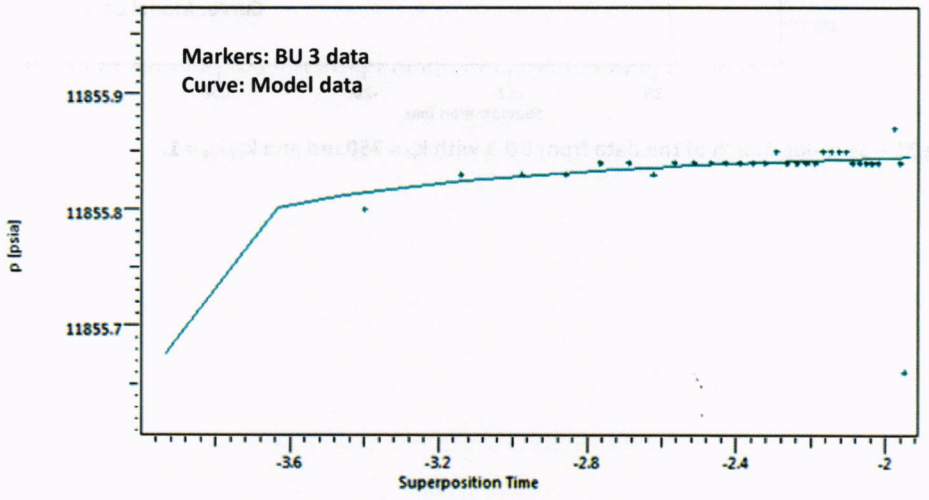

Figure 70 – Semi-log match of the data from BU 3 with k_H = 250 md and k_V/k_H = 1.

A match of BU 3 with horizontal permeability 750 md is shown in the form of a semi-log plot in Figure 71 with k_V/k_H = 0.1 and skin value 0.9. This match is acceptable, but a match higher permeability is not likely. My impression is therefore that a permeability value near 500 md is a good estimate, but a higher value cannot be ruled out on the basis of MDT data.

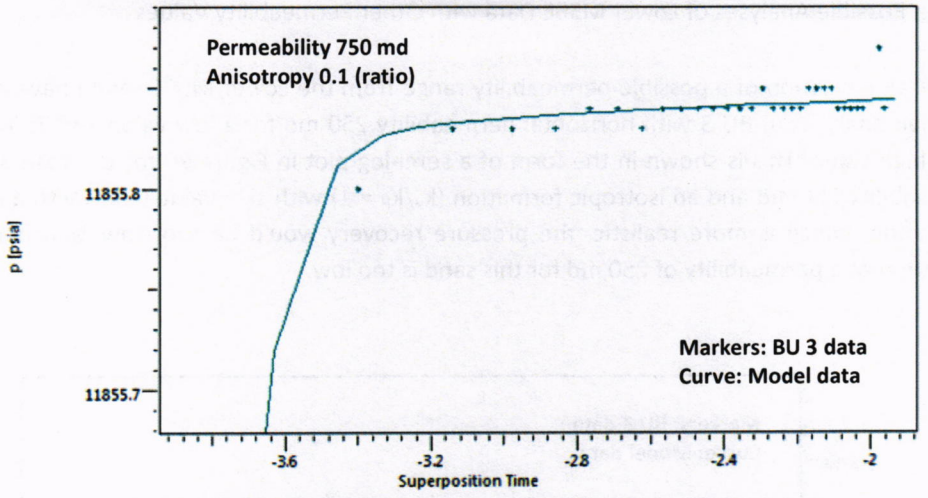

Figure 71 – Semi-log match of the data from BU 3 with k_H = 750 md and k_V/k_H = 1.

9. INFORMATION REQUIRED BY THE FEDERAL RULES OF CIVIL PROCEDURE

This report contains my opinions, conclusions, and reasons therefore.

A general statement of my qualifications is contained in the Professional Background section, page 3. A more detailed statement of my qualifications is included in Appendix A.

A list of publications since 1993 is provided in Appendix A.

The compensation to Kappa Engineering for my time preparing this report and any testimony as an expert witness at trial or deposition is as follows: $ 475 per hour.

I have not testified as an expert witness before.

The facts and data I considered in forming my opinions are listed in Appendix B.

The opinions expressed in this report are my own and are based on the data and facts available to me at the time of writing. Should additional relevant or pertinent information become available, I reserve the right to supplement the discussion and findings in this report.

APPENDIX A – CV LEIF LARSEN

CURRICULUM VITAE

Name:	Leif Larsen
Consultant:	Reservoir Engineering, Well Test Analysis
E-mail:	larsen@kappaeng.com (Kappa Engineering)
E-mail:	[redacted] (private)
E-mail:	leif.larsen@uis.no (University in Stavanger)
Private Address:	[redacted]
Telephone:	(47) 51 65 66 04.
Mobile:	[redacted]
Born:	[redacted]
Citizenship:	Norwegian.
Family situation:	Married to Brit Eva Larsen.
Children:	4
Education:	Examen artium (high school), Stavanger Katedralskole, 1965.
	Bachelor of Arts in Mathematics, University of California, Irvine, 1969.
	Doctor of Philosophy in Mathematics, Univ. of California, Irvine, 1975.

Courses in Petroleum Technology:

Well Testing, R. Raghavan, Rogaland College Center, 1980 (2 weeks).
Principles of Well Testing, J.R. Bergeson and Associates, London, 1983 (1 week).
Advanced Well Testing, J.R. Bergeson and Associates, London, 1983 (1 week).
Naturally Fractured Reservoirs, R. Aguilera, Dallas, 1983 (1 week).

Professional Experience:

Teaching Assistant, Math. Dept., Univ. of California, Irvine, 1969 - 1972.
Research Assistant, Math. Dept., Univ. of California, Irvine, 1972 - 1973.
Teaching Assistant, Math. Dept., Univ. of California, Irvine, 1973 - 1975.
Teaching Assistant, Math. Dept., University of Oslo, 1975 - 1976.
Amanuensis in Mathematics, Agder Regional College, 1977 - 1979.
Amanuensis in Mathematics, Rogaland College Center, 1979 - 1980.
Researcher, Sector for Petroleum Tech., Rogaland Research Inst., 1980 -1985.
Consultant (1/5 position), Section for Special Studies, Reservoir Technology, Statoil, 1985 - 1988.
Research Supervisor, Sector for Petroleum Technology, Rogaland Research Inst., 1985 - 1991.
Staff Engineer, Reservoir Technology, Statoil, 1991 - 1993.
Staff Engineer, Production Technology, Statoil, 1993 – 2002.
Specialist Well Testing, Production Technology, Statoil, 2002 – Dec. 31, 2007.
Senior Reservoir Engineer (Consultant), Kappa Engineering, Jan. 1, 2008 – present.

Adjunct Professor (Professor II), Petroleum Technology, University in Stavanger, 1987 - present.

Memberships:

American Mathematical Society, Institutional Nominee, 1971 - 1981.
Society of Petroleum Engineers, 1981 - present.

Courses Taught in Petroleum Technology:

Well Analysis, cand. techn., Stavanger University Center, 1983 - 1984.
Well Test Analysis, Statoil, 1984 and 1986.
Well Test Analysis, University in Stavanger, 1981 - present.

Activities for SPE:

Technical Advisor (referee), 1983 - 1984.
Technical Editor, 1984 - 1992.
Member of the Pressure Transient Testing Technical Committee, 1988 - 1989.

Member of the Program Committee for the SPE Forum Series in Europe, *Advances in Well Test Design & Interpretation*, Seefeld, Sept. 1992.
Member of the Pressure Transient Testing Technical Committee, 1995 - 2005.
SPE Distinguished Lecturer, 1998 - 1999, *Performance Prediction and Testing of Multilateral and Horizontal Wells*.
Member of the Pressure Transient Testing Special Reprint Committee, 2004.
Committee Member of several SPE ATW's.

Interests and hobbies: Outdoors activities.

***Publications in Mathematics*:**

1. Larsen, Leif: "Hierarchies of Computational Groups and the Conjugacy Problem," Ph.D. thesis, University of California, Irvine, 1975.
2. Larsen, Leif: "The Solvability of the Conjugacy Problem for Certain Free Groups With Amalgamation," *J. Algebra*, (1976), 28-41.
3. Larsen, Leif: "The Conjugacy Problem and Cyclic HNN Constructions," *J. Austral. Math. Soc.* Vol. 23 No. 4 (1977), 385-401.
4. Larsen, Leif: "On the Computability of Conjugate Powers in Finitely Generated Fuchsian Groups," *Acta Mathematica*, 139 (1977), 267-291.
5. Larsen, Leif: "Decision Problems and Minimal Identities in Groups," preprint, Agder Regional College, 1979.

***Publications in Petroleum Technology*:**

1. Larsen, Leif: "Wells Producing Commingled Zones With Unequal Initial Pressure and Reservoir Properties," paper SPE 10325 presented at the 1981 SPE Annual Technical Conference and Exhibition, San Antonio, Oct. 5-7. (Accepted for publication in *Soc. Pet. Eng. J.*)
2. Larsen, Leif: "Determination of Skin Factors and Flow Capacities of Individual Layers in Two-Layered Reservoirs," paper SPE 11138 presented at the 1982 SPE Annual Technical Conference and Exhibition, New Orleans, Sept. 26-29.
3. Larsen, Leif: "Limitations on the Use of Single- and Multiple-Rate Horner, Miller- Dyes-Hutchinson, and Matthews-Brons-Hazebroek Analysis," paper SPE 12135 presented at the 1983 SPE Annual Technical Conference and

Exhibition, San Fransisco, Oct. 5-8. (Accepted for publication in *Soc. Pet. Eng. J.*)

4. Larsen, Leif: "Wellbore Pressure Near Closed Boundaries," unsolicited paper SPE 11861 (Accepted for publication in *Soc. Pet. Eng. J.*)

5. Haugland, T., Larsen, L., and Skjæveland, S.M.: "Analyzing Pressure Buildup Data by the Rectangular Hyperbola Approach," paper SPE 13079 presented at the 1984 SPE Annual Technical Conference and Exhibition, Houston, Sept. 16-19. (Accepted for publication in *SPEFE*)

6. Larsen, Leif: "Wellbore Pressures in Reservoirs With Constant-Pressure or Mixed No-Flow/Constant-Pressure Outer Boundary," *JPT* (Sept. 1984) 1613-1616.

7. Larsen, Leif: "A Simple Approach to Pressure Distributions in Geometric Shapes," *Soc. Pet. Eng. J.* (Feb. 1985) 113-120.

8. Litlehamar, Terje and Larsen, Leif: "Matching Simulator Well-Block Pressures With Observed Buildup Pressures in Two-Layer Reservoirs," *SPERE* (March 1986) 183-193.

9. Larsen, Leif: "Cumulative Influx Across Constant-Pressure Boundaries of Rectangular Reservoirs and Its Effect of Well-Test Analysis," *North Sea Oil and Gas Reservoirs: An International Seminar*, Kleppe, J., *et al.*, eds., Graham & Trotman Ltd., London. 1987.

10. Larsen, Leif and Hovdan, Michael: "Analyzing Well-Test Data From Linear Reservoirs by Conventional Methods," paper SPE 16777 presented at the 1987 SPE Annual Technical Conference and Exhibition, Dallas, Sept. 27-30. (Accepted for publication in *SPEPE.*)

11. Larsen, Leif: "Similarities and Differences in Methods Currently Used to Analyze Pressure-Transient Data From Layered Reservoirs," paper SPE 18122 presented at the 1988 SPE Annual Technical Conference and Exhibition, Houston, Oct. 5-7.

12. Larsen, Leif: "Boundary Effects in Pressure-Transient Data From Layered Reservoirs," paper SPE 19797 presented at the 1989 SPE Annual Technical Conference and Exhibition, San Antonio, Oct. 8-11. (Accepted for publication in *SPEFE.*)

13. Larsen, L. and Bratvold, R.B.: "Effects of Linear Boundaries on Pressure-Transient Injection and Falloff Data," paper SPE 19830 presented at the 1989 SPE Annual Technical Conference and Exhibition, San Antonio, Oct. 8-11.

14. Larsen, Leif and Kviljo, Knut: "Variable Skin and Cleanup Effects in Well-Test Data," *SPEFE* (Sept. 1990) 272-276.

15. Larsen, L., Kviljo, K., and Litlehamar, T.: "Estimating Skin Decline and Relative Permeabilities From Cleanup Effects in Well-Test Data Using Buckley-Leverett Methods," *SPEFE* (Dec. 1990) 360-368.

16. Larsen, L. and Hegre, T.M.: "Pressure-Transient Behavior of Horizontal Wells With Finite-Conductivity Fractures," paper SPE 22076 presented at the 1991 International Arctic Technology Conference, Anchorage, May 29-31.

17. Larsen, Leif: "Pressure-Transient Behavior of Reservoirs Forming a Pattern of Coupled Linear Segments," paper SPE 26459 presented at the 1993 SPE Annual Technical Conference and Exhibition, Houston, Oct. 3-6.

18. Larsen, Leif: "The Pressure-Transient Behavior of Vertical Wells With Multiple Flow Entries," paper SPE 26480 presented at the 1993 SPE Annual Technical Conference and Exhibition, Houston, Oct. 3-6.

19. Larsen, L. and Bratvold, R.B.: "Effects of Propagating Fractures on Pressure-Transient Injection and Falloff Data," *SPEFE* (June 1994) 105-114.

20. Larsen, Leif: "Experiences With Combined Analyses of PLT and Pressure-Transient Data From Layered Reservoirs," paper SPE 27973 presented at the 1994 Tulsa Centennial Petroleum Engineering Symposium, Tulsa, Aug. 29-31.

21. Larsen, L. and Hegre, T.M.: "Pressure Transient Analysis of Multifractured Horizontal Wells," paper SPE 28389 presented at the 1994 SPE Annual Technical Conference and Exhibition, New Orleans, Sept. 25-28.

22. Hegre, T.M. and Larsen, L.: "Productivity of Multifractured Horizontal Wells," paper SPE 28845 presented at the 1994 European Petroleum Conference, London, Oct. 25-27.

23. Unneland, Trond and Larsen, Leif: "Limitations of the Skin Concept and Its Impact on Success Criteria Used in Sand Control," paper SPE 30093 presented at the 1995 European Formation Damage Conference, The Hague, May 15-16.

24. Larsen, Leif: "Pressure-Transient Behavior of Wells Producing From a Complex Pattern of Interconnected Linear Segments," paper SPE 36549 presented at the 1996 SPE Annual Technical Conference and Exhibition, Denver, Oct. 6-9.

25. Larsen, Leif: "Productivity Computations for Multilateral, Branched and Other Generalized and Extended Well Concepts," paper SPE 36754 presented at the 1996 SPE Annual Technical Conference and Exhibition, Denver, Oct. 6-9.

26. Larsen, Leif: "Determination of Pressure-Transient and Productivity Data for Deviated Wells in Layered Reservoirs," *SPERE* (Feb. 1999) 95-103.

27. Larsen, Leif: "Productivities of Fractured and Nonfractured Deviated Wells in Commingled Layered Reservoirs," *SPEJ* (June 1998) 191-199.

28. Larsen, Leif: "Pressure-Transient Behavior of Multibranched Wells in Layered Reservoirs," *SPERE* (Feb. 2000) 68-73.

29. Jensen, B., Fougner, A.H., and Larsen, L.: "Interference Testing to Verify Drainage Strategy for a Large Offshore Development," paper SPE 56420 presented at the 1999 SPE Annual Technical Conference and Exhibition, Houston, Oct. 3-6.

30. Nilsen, F. and Larsen, L.: "Inflow Predictions and Testing While Underbalanced Drilling," paper SPE 56684 presented at the 1999 SPE Annual Technical Conference and Exhibition, Houston, Oct. 3-6.

31. Bale, A., Larsen, L., Tudor, D.T., and Buchanan, A.: "Propped Fracturing as a Tool for Prevention and Removal of Formation Damage," paper SPE 68913 presented at the 2001 SPE European Formation Damage Conference, The Hague, May 21-22.

32. Larsen, L.: "General Productivity Models for Wells in Homogeneous and Layered Reservoirs," paper SPE 71613 presented at the 2001 SPE Annual Technical Conference and Exhibition, New Orleans, Sept. 30-Oct. 3.

33. Larsen, L.: "Uncertainties in Standard Analyses of Boundary Effects in Buildup Data," *SPEREE* (Oct. 2005) 437-444.

34. Larsen, L.: "Modeling and Analyzing Source and Interference Data From Packer-Probe and Multiprobe Tests," paper SPE 102698 presented at the 2006 SPE Annual Technical Conference and Exhibition, San Antonio, Sept. 24-27.

35. Larsen, L.: "Boundary Effects and Depth of Investigation From Long Buildups Following Short Flow Tests," paper SPE 102699 presented at the 2006 SPE Annual Technical Conference and Exhibition, San Antonio, Sept. 24-27.

36. Larsen, L. and Straub, R.B.: "Determination of Connected Volume and Connectivity From Extended Tests in Compartmentalized and Layered Reservoirs," paper SPE 110011 presented at the 2007 SPE Annual Technical Conference and Exhibition, Anaheim, California, Nov. 11-14.

37. Larsen, L.: "Analyzing Buildup Data Following a Highly Unstable Rate History," paper SPE 106738 presented at the 2008 SPE Annual Technical Conference and Exhibition, Denver, Colorado, Sept. 21-24.

38. Larsen, L.: "Horizontal Fractures in Single and Multilayer Reservoirs," paper CSUG/SPE 147004 presented at the 2011 Canadian Unconventional Resources Conference, Calgary, Alberta, Canada, 15–17 November, 2011.

APPENDIX B – FACTS AND DATA CONSIDERED IN FORMING MY OPINION

BP_MC252_OCSG_32306_001_ST00BP01_R1D4_MDT_OFA_143LTP.las
BP_MC252_OCSG_32306_001_ST00BP01_R1D4_MDT_OFA_144LTP.las
BP_MC252_OCSG_32306_001_ST00BP01_R1D4_MDT_OFA_147LTP.las

Expert report of Alain Gringarten, May 1, 2013

Schlumberger MDT Report, 9-May-2010 (file: 108369501[1].pdf)

71b_WFT-MDL-00070780.xls
20100419_2130_WTH006-7346-7348.xls
BPD568-97605-97605.xls

BP-HZN-BLY00082877
BP-HZN-BLY00082886
BP-HZN-BLY00082887
BP-HZN-BLY00082889
BP-HZN-BLY00082890
BP-HZN-BLY00082891
BP-HZN-BLY00082892
BP-HZN-BLY00082893
BP-HZN-BLY00082894
BP-HZN-BLY00082895
BP-HZN-BLY00082896
BP-HZN-BLY00082897
BP-HZN-BLY00082898
BP-HZN-BLY00082899
BP-HZN-BLY00082900
BP-HZN-BLY00082901
BP-HZN-BLY00082902
BP-HZN-BLY00082903

Emanuel Deposition